

# GRAFIQS: Face Image Quality Assessment Using Gradient Magnitudes

## Supplementary Material

Jan Niklas Kolf<sup>1,2</sup>, Naser Damer<sup>1,2</sup>, Fadi Boutros<sup>1</sup>

<sup>1</sup>Fraunhofer Institute for Computer Graphics Research IGD, Germany

<sup>2</sup>Technical University of Darmstadt, Germany

{jan.niklas.kolf, naser.damer, fadi.boutros}@igd.fraunhofer.de

### 1. Supplementary Material

This supplementary material contains the following supporting content:

- An ablation on a different backbone (ResNet50 [4]): To validate the generalizability over different backbones, we present in Table 1 the achieved AUC over the utilized benchmarks and FR models, similar to Table 2 in the main paper, that shows the AUC for the ResNet100 backbone. Similar to Figure 2 in the main paper, Figures 1, 2, 3, 4, 5, 6, 7 show the EDC curves achieved by our  $MSE_{BNS}$  and  $\mathcal{L}_{BNS}$  approaches on datasets Adience, AgeDB30, CFP-FP, LFW, CALFW, CPLFW, and XQLFW for all utilized FR models, respectively.
- Due to limited space in the main paper, we present here all EDC figures of ResNet100 backbone over all utilized datasets and FR models. Figures 8, 9, 10, 11, 12, 13, 14 show the EDC curves achieved by our  $MSE_{BNS}$  and  $\mathcal{L}_{BNS}$  approaches on datasets Adience, AgeDB30, CFP-FP, LFW, CALFW, CPLFW, and XQLFW for all utilized FR models, respectively.
- Furthermore we provide all EDC figures that show a comparison between GRAFIQS using ResNet100, reported using the best setting from Table 2 in the main paper, and SOTA methods. Figures 15, 16, 17, 18, 19, 20, 21 show the EDC curves on datasets Adience, AgeDB30, CFP-FP, LFW, CALFW, CPLFW, and XQLFW for all utilized FR models, respectively.

FR	Loss $\mathcal{L}$	FIQ	Gradient	Adience [3]		AgeDB30 [9]		CFP-FP [10]		LFW [5]		CALFW [12]		CPLFW [11]		XQLFW [7]		Mean AUC	
				$1e-3$	$1e-4$	$1e-3$	$1e-4$	$1e-3$	$1e-4$	$1e-3$	$1e-4$	$1e-3$	$1e-4$	$1e-3$	$1e-4$	$1e-3$	$1e-4$	$1e-3$	$1e-4$
ArcFace [2]	-	MSE(BNS <sub>M</sub> , BNS <sub>T</sub> )	-	0.0311	0.0668	0.0337	0.0470	0.0204	0.0266	0.0034	0.0041	0.0665	0.0700	0.0630	0.0903	0.2436	0.2946	0.0660	0.0856
	$\mathcal{L}_{BNS}$	$\sum \partial \mathcal{L} / \partial \phi$	$\phi = \mathcal{I}$	0.0262	0.0527	0.0312	0.0412	0.0126	0.0199	0.0034	0.0041	0.0637	0.0679	0.0552	0.0867	0.2382	0.2896	0.0615	0.0803
	$\mathcal{L}_{BNS}$	$\sum \partial \mathcal{L} / \partial \phi$	$\phi = B1$	0.0261	0.0523	0.0288	0.0385	0.0137	0.0236	0.0033	0.0040	0.0673	0.0725	0.0588	0.0898	0.2370	0.2925	0.0621	0.0819
	$\mathcal{L}_{BNS}$	$\sum \partial \mathcal{L} / \partial \phi$	$\phi = B2$	0.0258	0.0522	0.0286	0.0377	0.0142	0.0235	0.0028	0.0036	0.0732	0.0786	0.0607	0.0927	0.2409	0.2905	0.0637	0.0827
	$\mathcal{L}_{BNS}$	$\sum \partial \mathcal{L} / \partial \phi$	$\phi = B3$	0.0289	0.0606	0.0308	0.0417	0.0279	0.0377	0.0028	0.0035	0.0771	0.0833	0.1125	0.1420	0.3638	0.4054	0.0920	0.1106
$\mathcal{L}_{BNS}$	$\sum \partial \mathcal{L} / \partial \phi$	$\phi = B4$	0.0245	0.0510	0.0248	0.0368	0.0181	0.0285	0.0041	0.0046	0.0582	0.0650	0.0595	0.0893	0.2441	0.2761	0.0619	0.0788	
ElasticFace [1]	-	MSE(BNS <sub>M</sub> , BNS <sub>T</sub> )	-	0.0335	0.0631	0.0314	0.0329	0.0194	0.0243	0.0031	0.0041	0.0628	0.0651	0.0572	0.0754	0.2143	0.2583	0.0602	0.0747
	$\mathcal{L}_{BNS}$	$\sum \partial \mathcal{L} / \partial \phi$	$\phi = \mathcal{I}$	0.0280	0.0505	0.0328	0.0360	0.0118	0.0152	0.0032	0.0041	0.0620	0.0638	0.0549	0.0705	0.2160	0.2445	0.0584	0.0692
	$\mathcal{L}_{BNS}$	$\sum \partial \mathcal{L} / \partial \phi$	$\phi = B1$	0.0279	0.0503	0.0313	0.0347	0.0127	0.0160	0.0031	0.0040	0.0647	0.0667	0.0556	0.0837	0.2168	0.2468	0.0589	0.0717
	$\mathcal{L}_{BNS}$	$\sum \partial \mathcal{L} / \partial \phi$	$\phi = B2$	0.0278	0.0500	0.0317	0.0353	0.0132	0.0165	0.0027	0.0036	0.0711	0.0732	0.0577	0.0852	0.2183	0.2555	0.0604	0.0742
	$\mathcal{L}_{BNS}$	$\sum \partial \mathcal{L} / \partial \phi$	$\phi = B3$	0.0311	0.0571	0.0358	0.0395	0.0244	0.0320	0.0026	0.0035	0.0748	0.0763	0.1044	0.1536	0.3376	0.3845	0.0872	0.1066
$\mathcal{L}_{BNS}$	$\sum \partial \mathcal{L} / \partial \phi$	$\phi = B4$	0.0262	0.0488	0.0258	0.0280	0.0139	0.0183	0.0039	0.0046	0.0556	0.0578	0.0546	0.0693	0.2012	0.2416	0.0545	0.0669	
MagFace [8]	-	MSE(BNS <sub>M</sub> , BNS <sub>T</sub> )	-	0.0326	0.0663	0.0329	0.0699	0.0305	0.0486	0.0041	0.0049	0.0664	0.0682	0.0627	0.1414	0.2727	0.3274	0.0717	0.1038
	$\mathcal{L}_{BNS}$	$\sum \partial \mathcal{L} / \partial \phi$	$\phi = \mathcal{I}$	0.0276	0.0546	0.0339	0.0524	0.0188	0.0320	0.0035	0.0046	0.0648	0.0671	0.0601	0.1230	0.2654	0.3009	0.0677	0.0907
	$\mathcal{L}_{BNS}$	$\sum \partial \mathcal{L} / \partial \phi$	$\phi = B1$	0.0275	0.0550	0.0318	0.0504	0.0197	0.0318	0.0034	0.0045	0.0676	0.0700	0.0624	0.1460	0.2698	0.3119	0.0689	0.0957
	$\mathcal{L}_{BNS}$	$\sum \partial \mathcal{L} / \partial \phi$	$\phi = B2$	0.0274	0.0552	0.0319	0.0486	0.0206	0.0328	0.0029	0.0041	0.0736	0.0759	0.0673	0.1461	0.2728	0.3099	0.0709	0.0961
	$\mathcal{L}_{BNS}$	$\sum \partial \mathcal{L} / \partial \phi$	$\phi = B3$	0.0310	0.0631	0.0353	0.0529	0.0393	0.0584	0.0028	0.0040	0.0768	0.0798	0.1239	0.2893	0.4115	0.4721	0.1029	0.1457
$\mathcal{L}_{BNS}$	$\sum \partial \mathcal{L} / \partial \phi$	$\phi = B4$	0.0257	0.0525	0.0266	0.0540	0.0214	0.0376	0.0045	0.0060	0.0576	0.0597	0.0625	0.1123	0.2679	0.3092	0.0666	0.0902	
Curricular-Face [6]	-	MSE(BNS <sub>M</sub> , BNS <sub>T</sub> )	-	0.0284	0.0583	0.0313	0.0388	0.0215	0.0280	0.0035	0.0041	0.0659	0.0698	0.0529	0.0798	0.1916	0.2380	0.0564	0.0738
	$\mathcal{L}_{BNS}$	$\sum \partial \mathcal{L} / \partial \phi$	$\phi = \mathcal{I}$	0.0249	0.0459	0.0330	0.0387	0.0140	0.0194	0.0034	0.0041	0.0628	0.0659	0.0499	0.0752	0.1988	0.2275	0.0553	0.0681
	$\mathcal{L}_{BNS}$	$\sum \partial \mathcal{L} / \partial \phi$	$\phi = B1$	0.0248	0.0457	0.0305	0.0358	0.0149	0.0197	0.0033	0.0040	0.0646	0.0675	0.0509	0.0909	0.2036	0.2288	0.0561	0.0703
	$\mathcal{L}_{BNS}$	$\sum \partial \mathcal{L} / \partial \phi$	$\phi = B2$	0.0246	0.0455	0.0306	0.0361	0.0153	0.0198	0.0029	0.0036	0.0703	0.0731	0.0516	0.0912	0.2029	0.2320	0.0569	0.0716
	$\mathcal{L}_{BNS}$	$\sum \partial \mathcal{L} / \partial \phi$	$\phi = B3$	0.0274	0.0512	0.0333	0.0401	0.0294	0.0335	0.0030	0.0037	0.0735	0.0765	0.0981	0.1657	0.3322	0.3716	0.0853	0.1060
$\mathcal{L}_{BNS}$	$\sum \partial \mathcal{L} / \partial \phi$	$\phi = B4$	0.0230	0.0438	0.0253	0.0299	0.0170	0.0195	0.0041	0.0046	0.0572	0.0600	0.0495	0.0710	0.2204	0.2639	0.0566	0.0704	

Table 1. The achieved AUC of EDC by using two approaches presented in this paper, MSE of BNS (MSE<sub>BNS</sub>) and gradient magnitudes ( $\mathcal{L}_{BNS}$ ), and under different settings. The ResNet50 model is used. The gradient magnitudes are extracted during the backpropagation step from different intermediate layers, B1, B2, B3 and B4 ( $\phi = B1 - \phi = B4$ ) as well as on the pixel level ( $\phi = \mathcal{I}$ ). The results are reported under two operation threshold  $FMR = 1e-3$  and  $FMR = 1e-4$  and under two protocols, same model (ArcFace) and cross-model (ElasticFace, MagFace and CurricularFace).

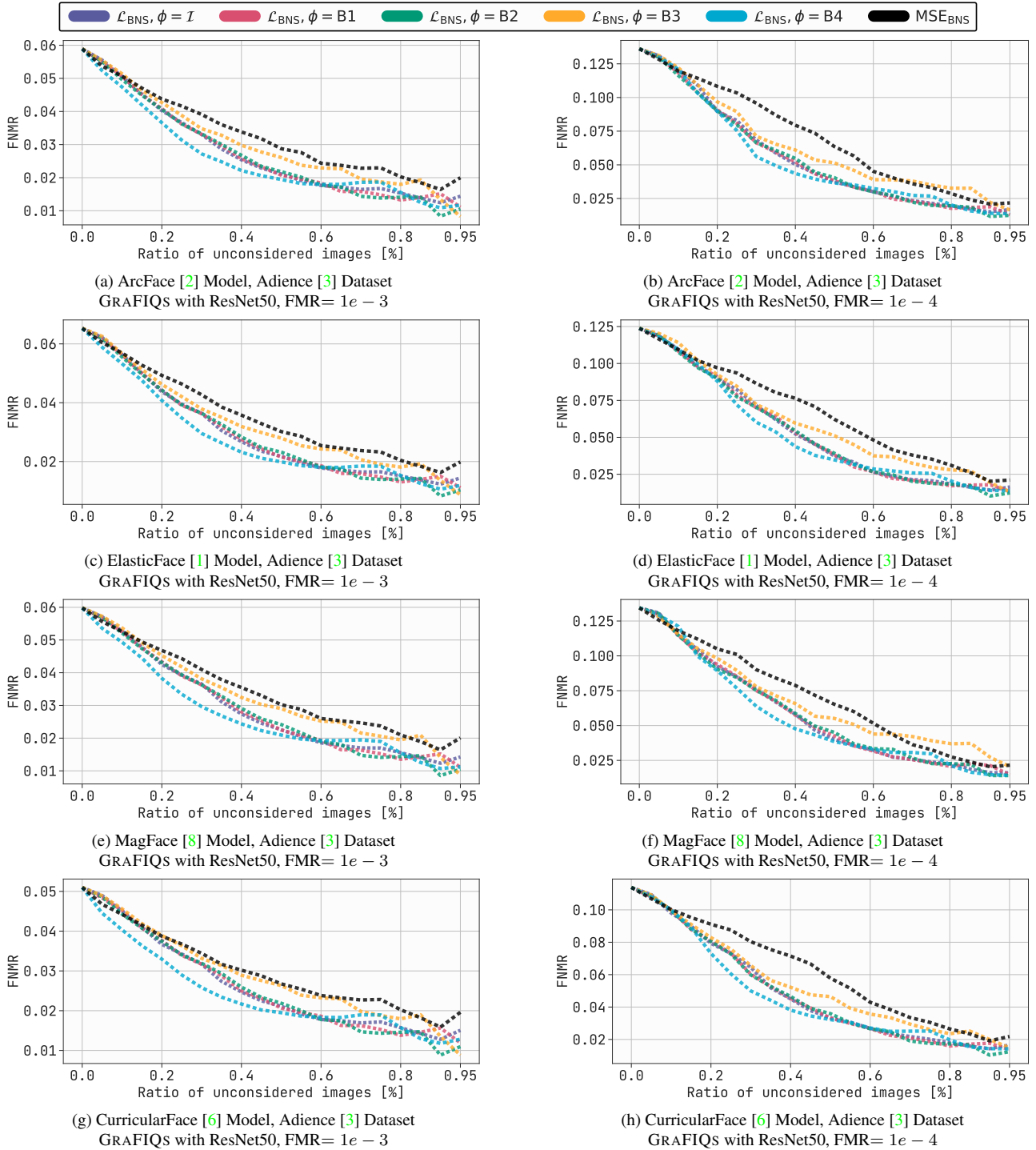


Figure 1. Error-versus-Discard Characteristic (EDC) curves for  $\text{FNMR}@FMR=1e-3$  and  $\text{FNMR}@FMR=1e-4$  of our proposed method using  $\mathcal{L}_{\text{BNS}}$  as backpropagation loss and absolute sum as FIQ. The gradients at image level ( $\phi = \mathcal{I}$ ), and block levels ( $\phi = \text{B1} - \phi = \text{B4}$ ) are used to calculate FIQ.  $\text{MSE}_{\text{BNS}}$  as FIQ is shown in black. Results shown on benchmark Adience [3] using ArcFace, ElasticFace, MagFace, and, CurricularFace FR models. It is evident that the proposed GRAFIQs method leads to lower verification error when images with lowest utility score estimated from gradient magnitudes are rejected. Furthermore, estimating FIQ by backpropagating  $\mathcal{L}_{\text{BNS}}$  yields significantly better results than using  $\text{MSE}_{\text{BNS}}$  directly.

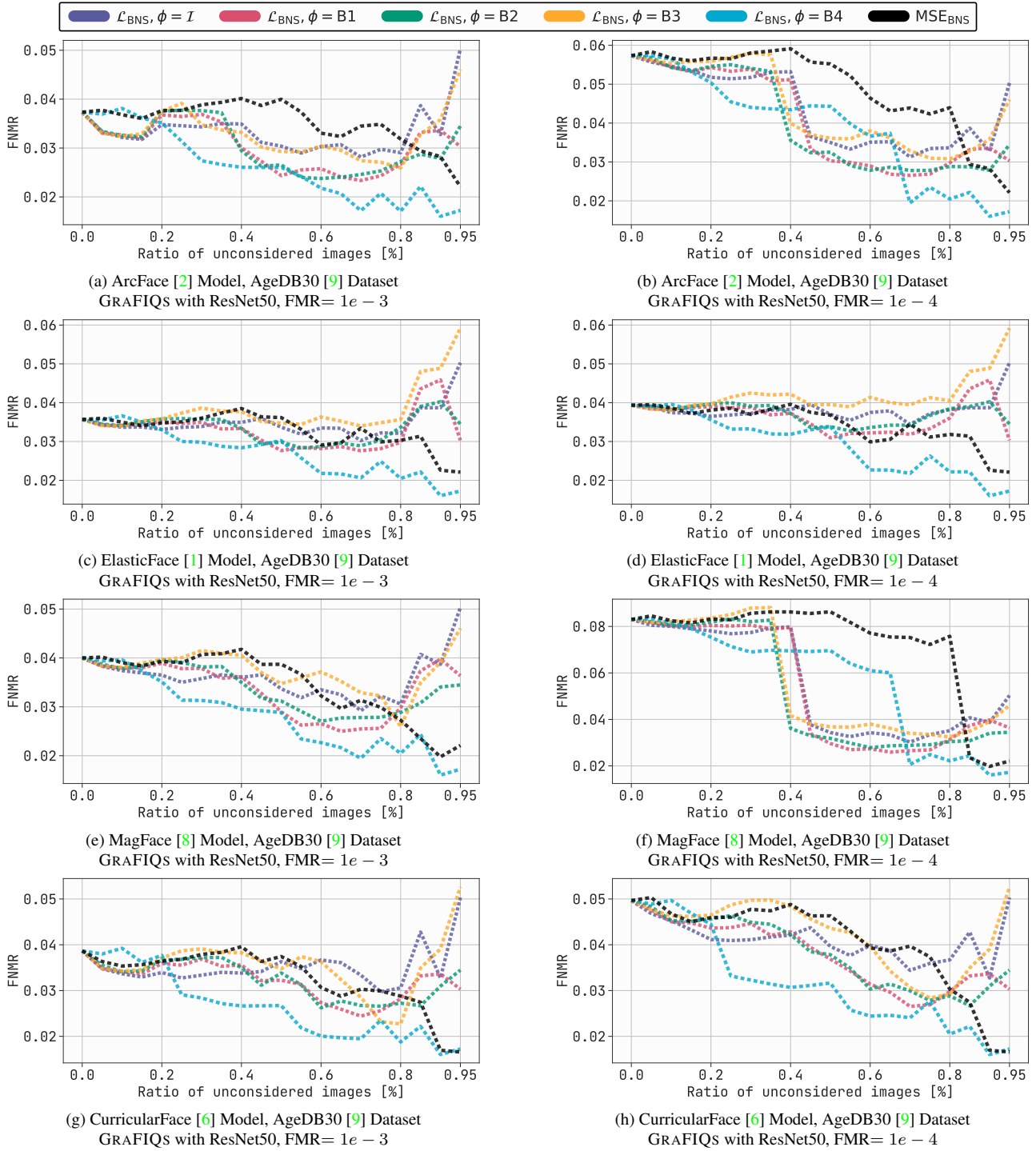


Figure 2. Error-versus-Discard Characteristic (EDC) curves for FNMR@FMR= $1e-3$  and FNMR@FMR= $1e-4$  of our proposed method using  $\mathcal{L}_{\text{BNS}}$  as backpropagation loss and absolute sum as FIQ. The gradients at image level ( $\phi = \mathcal{I}$ ), and block levels ( $\phi = \text{B1} - \phi = \text{B4}$ ) are used to calculate FIQ.  $\text{MSE}_{\text{BNS}}$  as FIQ is shown in black. Results shown on benchmark AgeDB30 [9] using ArcFace, ElasticFace, MagFace, and, CurricularFace FR models. It is evident that the proposed GRAFIQs method leads to lower verification error when images with lowest utility score estimated from gradient magnitudes are rejected. Furthermore, estimating FIQ by backpropagating  $\mathcal{L}_{\text{BNS}}$  yields significantly better results than using  $\text{MSE}_{\text{BNS}}$  directly.

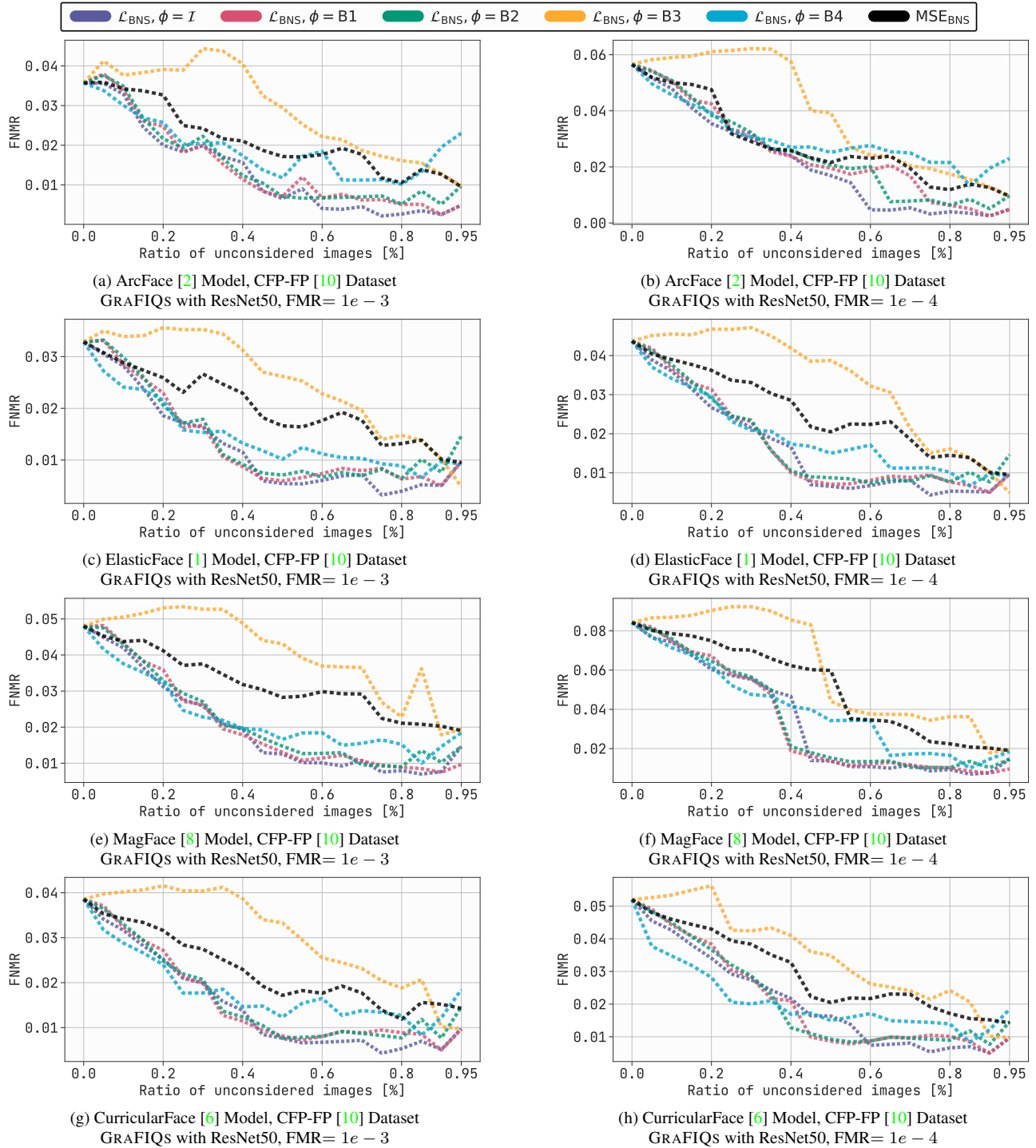


Figure 3. Error-versus-Discard Characteristic (EDC) curves for FNMR@FMR= $1e - 3$  and FNMR@FMR= $1e - 4$  of our proposed method using  $\mathcal{L}_{\text{BNS}}$  as backpropagation loss and absolute sum as FIQ. The gradients at image level ( $\phi = \mathcal{I}$ ), and block levels ( $\phi = \text{B1} - \phi = \text{B4}$ ) are used to calculate FIQ.  $\text{MSE}_{\text{BNS}}$  as FIQ is shown in black. Results shown on benchmark CFP-FP [10] using ArcFace, ElasticFace, MagFace, and, CurricularFace FR models. It is evident that the proposed GRAFIQS method leads to lower verification error when images with lowest utility score estimated from gradient magnitudes are rejected. Furthermore, estimating FIQ by backpropagating  $\mathcal{L}_{\text{BNS}}$  yields significantly better results than using  $\text{MSE}_{\text{BNS}}$  directly.

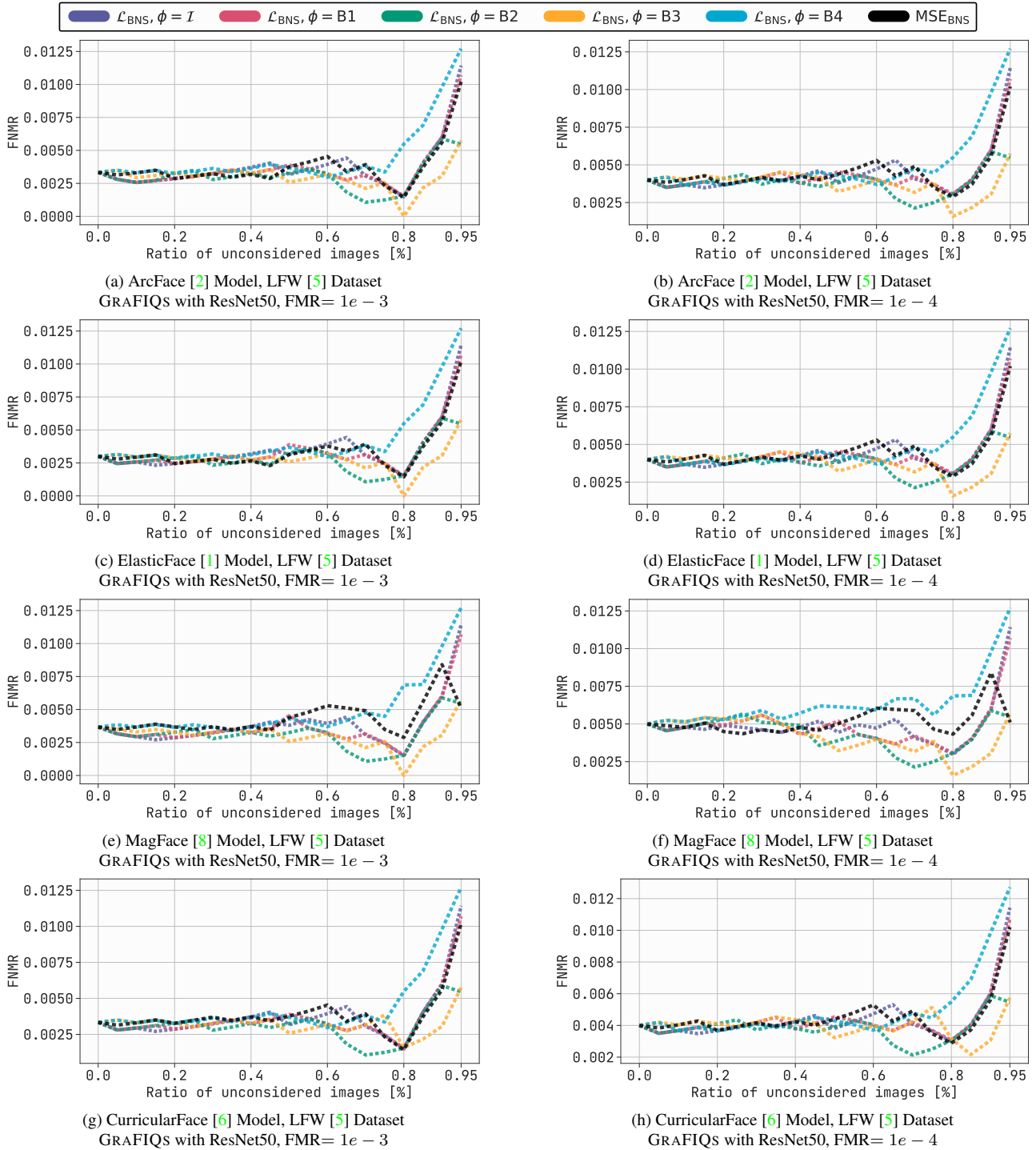


Figure 4. Error-versus-Discard Characteristic (EDC) curves for FNMR@FMR= $1e-3$  and FNMR@FMR= $1e-4$  of our proposed method using  $\mathcal{L}_{\text{BNS}}$  as backpropagation loss and absolute sum as FIQ. The gradients at image level ( $\phi = \mathcal{I}$ ), and block levels ( $\phi = \text{B1} - \phi = \text{B4}$ ) are used to calculate FIQ.  $\text{MSE}_{\text{BNS}}$  as FIQ is shown in black. Results shown on benchmark LFW [5] using ArcFace, ElasticFace, MagFace, and, CurricularFace FR models. It is evident that the proposed GRAFIQS method leads to lower verification error when images with lowest utility score estimated from gradient magnitudes are rejected. Furthermore, estimating FIQ by backpropagating  $\mathcal{L}_{\text{BNS}}$  yields significantly better results than using  $\text{MSE}_{\text{BNS}}$  directly.

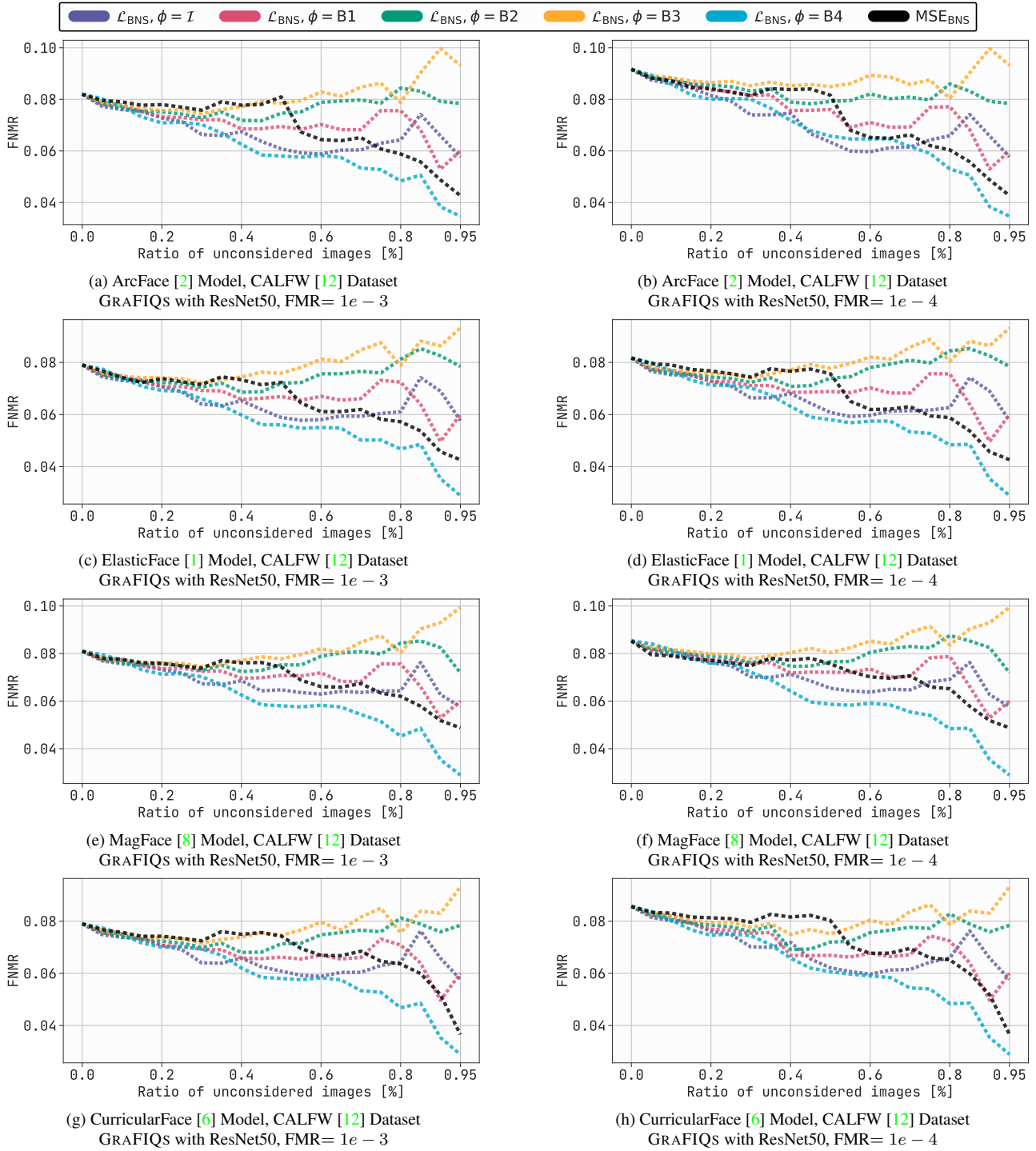


Figure 5. Error-versus-Discard Characteristic (EDC) curves for  $\text{FNMR}@FMR=1e-3$  and  $\text{FNMR}@FMR=1e-4$  of our proposed method using  $\mathcal{L}_{\text{BNS}}$  as backpropagation loss and absolute sum as FIQ. The gradients at image level ( $\phi = \mathcal{I}$ ), and block levels ( $\phi = \text{B1} - \phi = \text{B4}$ ) are used to calculate FIQ.  $\text{MSE}_{\text{BNS}}$  as FIQ is shown in black. Results shown on benchmark CALFW [12] using ArcFace, ElasticFace, MagFace, and, CurricularFace FR models. It is evident that the proposed GRAFIQS method leads to lower verification error when images with lowest utility score estimated from gradient magnitudes are rejected. Furthermore, estimating FIQ by backpropagating  $\mathcal{L}_{\text{BNS}}$  yields significantly better results than using  $\text{MSE}_{\text{BNS}}$  directly.

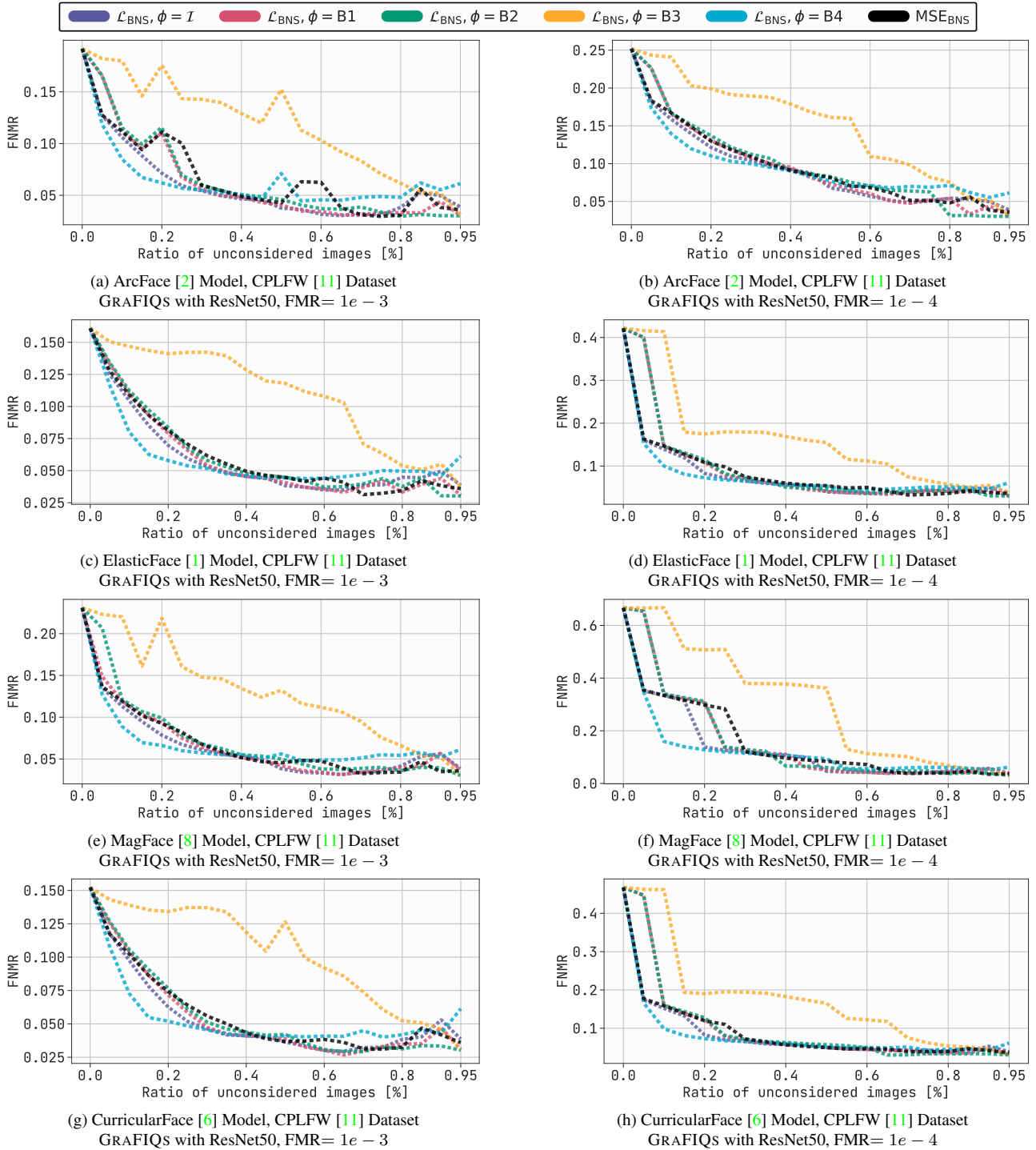


Figure 6. Error-versus-Discard Characteristic (EDC) curves for FNMR@FMR= $1e-3$  and FNMR@FMR= $1e-4$  of our proposed method using  $\mathcal{L}_{\text{BNS}}$  as backpropagation loss and absolute sum as FIQ. The gradients at image level ( $\phi = \mathcal{I}$ ), and block levels ( $\phi = \text{B1} - \phi = \text{B4}$ ) are used to calculate FIQ. MSE<sub>BNS</sub> as FIQ is shown in black. Results shown on benchmark CPLFW [11] using ArcFace, ElasticFace, MagFace, and, CurricularFace FR models. It is evident that the proposed GRAFIQS method leads to lower verification error when images with lowest utility score estimated from gradient magnitudes are rejected. Furthermore, estimating FIQ by backpropagating  $\mathcal{L}_{\text{BNS}}$  yields significantly better results than using MSE<sub>BNS</sub> directly.



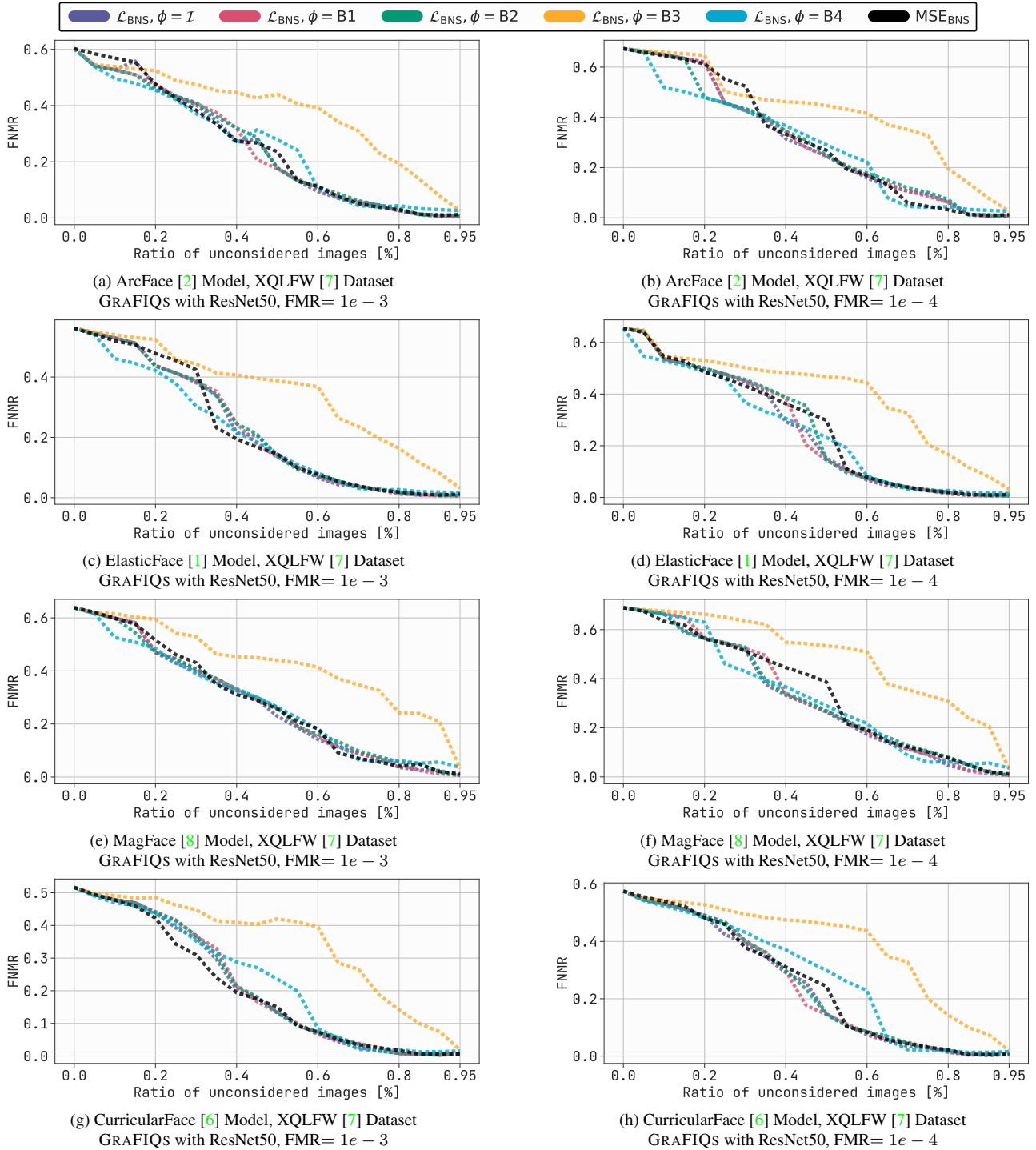


Figure 7. Error-versus-Discard Characteristic (EDC) curves for  $\text{FNMR}@FMR=1e-3$  and  $\text{FNMR}@FMR=1e-4$  of our proposed method using  $\mathcal{L}_{\text{BNS}}$  as backpropagation loss and absolute sum as FIQ. The gradients at image level ( $\phi = \mathcal{I}$ ), and block levels ( $\phi = \text{B1} - \phi = \text{B4}$ ) are used to calculate FIQ.  $\text{MSE}_{\text{BNS}}$  as FIQ is shown in black. Results shown on benchmark XQLFW [7] using ArcFace, ElasticFace, MagFace, and, CurricularFace FR models. It is evident that the proposed GRAFIQS method leads to lower verification error in most cases when images with lowest utility score estimated from gradient magnitudes are rejected. Furthermore, estimating FIQ by backpropagating  $\mathcal{L}_{\text{BNS}}$  yields on average better results than using  $\text{MSE}_{\text{BNS}}$  directly.

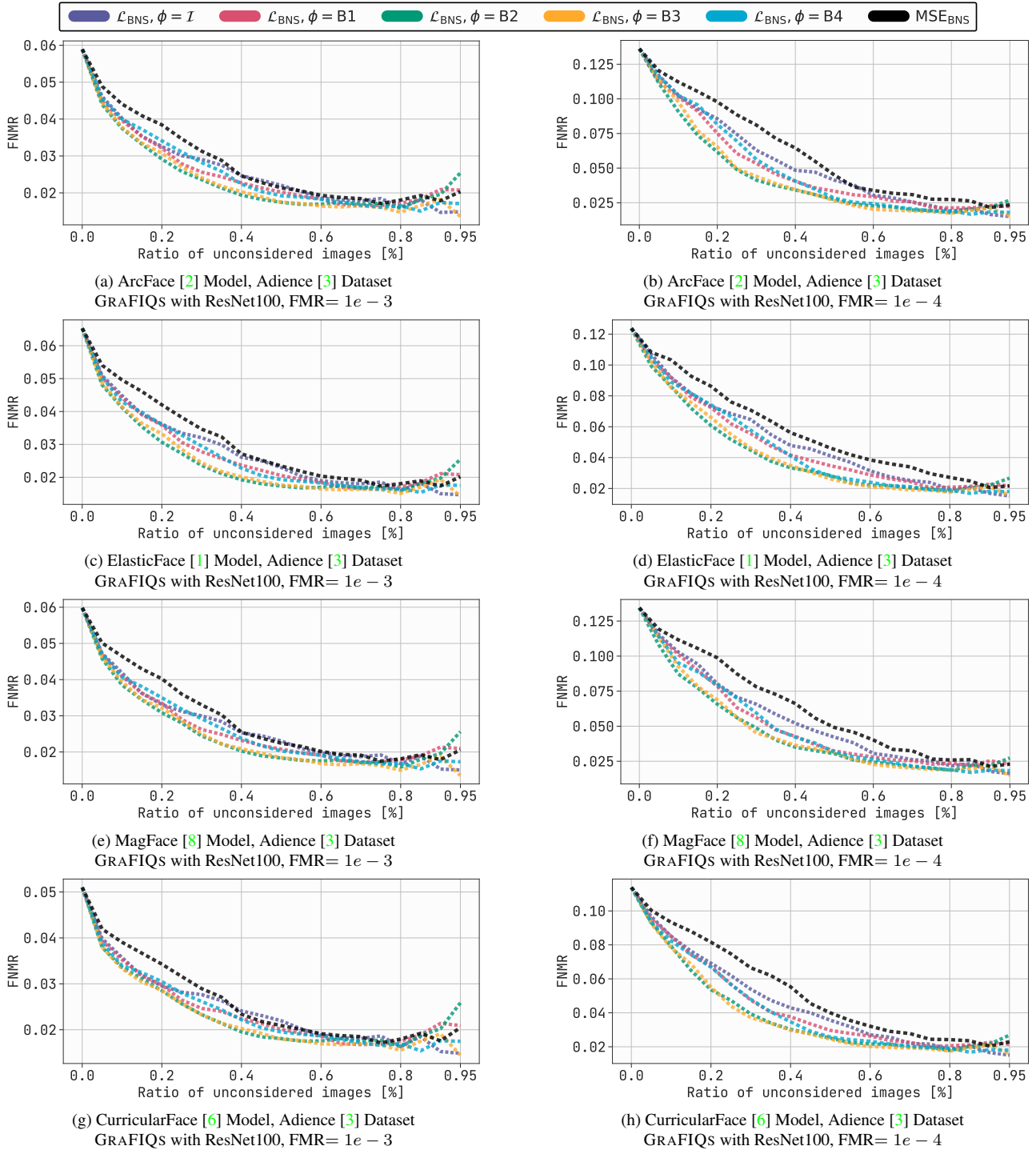


Figure 8. Error-versus-Discard Characteristic (EDC) curves for FNMR@FMR= $1e-3$  and FNMR@FMR= $1e-4$  of our proposed method using  $\mathcal{L}_{\text{BNS}}$  as backpropagation loss and absolute sum as FIQ. The gradients at image level ( $\phi = \mathcal{I}$ ), and block levels ( $\phi = \text{B1} - \phi = \text{B4}$ ) are used to calculate FIQ. MSE<sub>BNS</sub> as FIQ is shown in black. Results shown on benchmark Adience [3] using ArcFace, ElasticFace, MagFace, and, CurricularFace FR models. It is evident that the proposed GRAFIQS method leads to lower verification error when images with lowest utility score estimated from gradient magnitudes are rejected. Furthermore, estimating FIQ by backpropagating  $\mathcal{L}_{\text{BNS}}$  yields significantly better results than using MSE<sub>BNS</sub> directly.

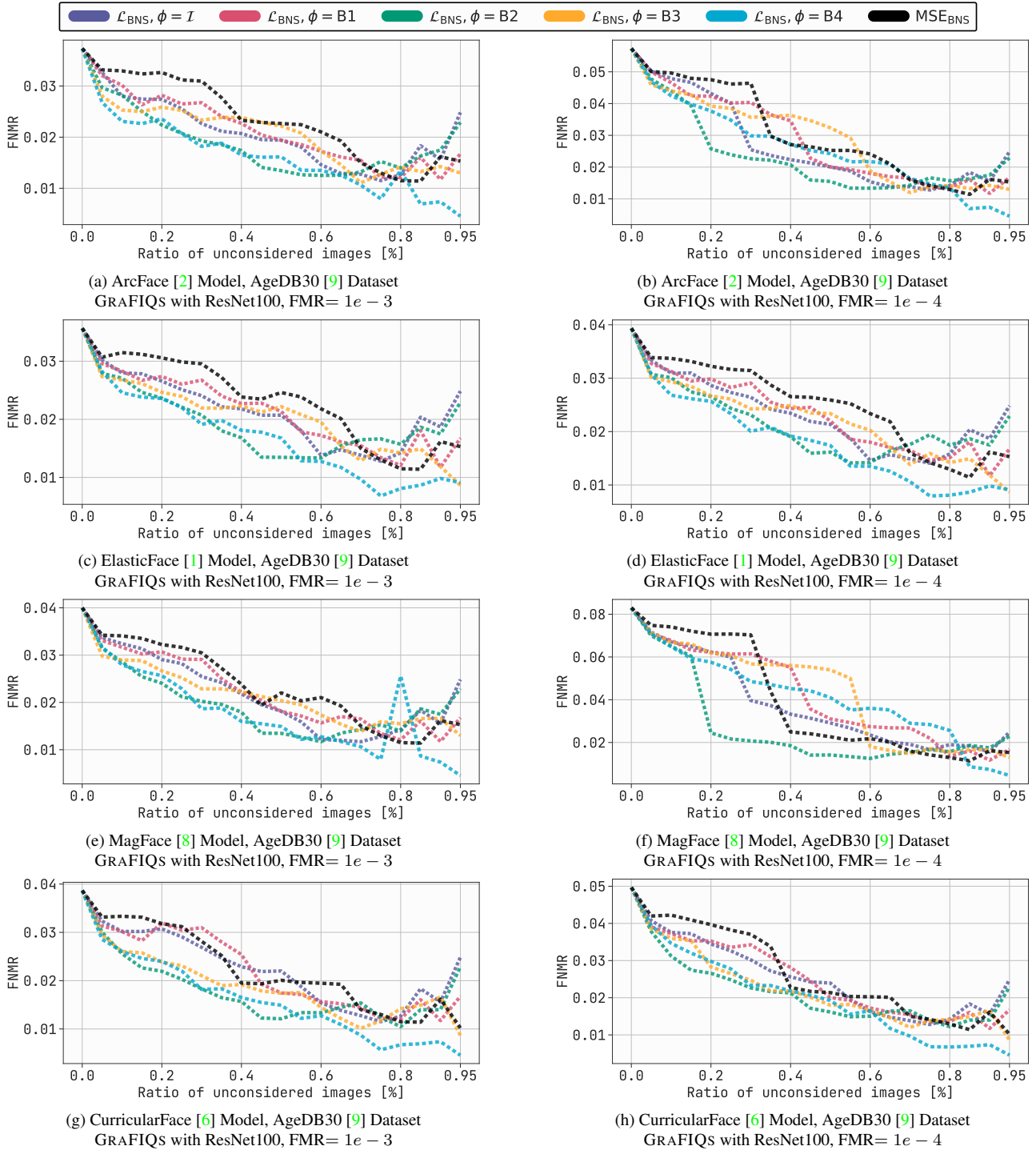


Figure 9. Error-versus-Discard Characteristic (EDC) curves for FNMR@FMR= $1e-3$  and FNMR@FMR= $1e-4$  of our proposed method using  $\mathcal{L}_{\text{BNS}}$  as backpropagation loss and absolute sum as FIQ. The gradients at image level ( $\phi = \mathcal{I}$ ), and block levels ( $\phi = \text{B1} - \phi = \text{B4}$ ) are used to calculate FIQ.  $\text{MSE}_{\text{BNS}}$  as FIQ is shown in black. Results shown on benchmark AgeDB30 [9] using ArcFace, ElasticFace, MagFace, and, CurricularFace FR models. It is evident that the proposed GRAFIQS method leads to lower verification error when images with lowest utility score estimated from gradient magnitudes are rejected. Furthermore, estimating FIQ by backpropagating  $\mathcal{L}_{\text{BNS}}$  yields significantly better results than using  $\text{MSE}_{\text{BNS}}$  directly.

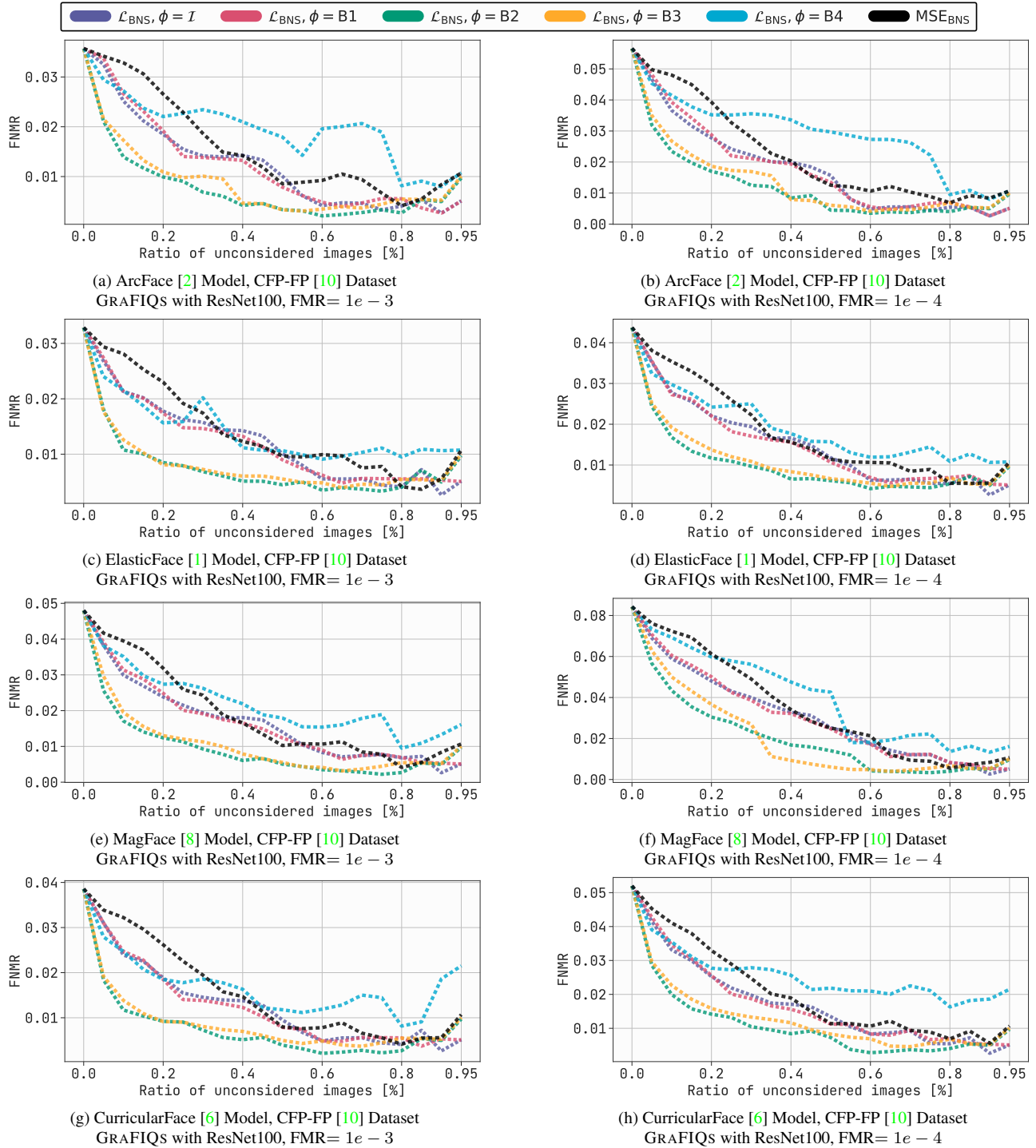


Figure 10. Error-versus-Discard Characteristic (EDC) curves for  $\text{FNMR}@FMR=1e-3$  and  $\text{FNMR}@FMR=1e-4$  of our proposed method using  $\mathcal{L}_{\text{BNS}}$  as backpropagation loss and absolute sum as FIQ. The gradients at image level ( $\phi = \mathcal{I}$ ), and block levels ( $\phi = \text{B1} - \phi = \text{B4}$ ) are used to calculate FIQ.  $\text{MSE}_{\text{BNS}}$  as FIQ is shown in black. Results shown on benchmark CFP-FP [10] using ArcFace, ElasticFace, MagFace, and, CurricularFace FR models. It is evident that the proposed GRAFIQS method leads to lower verification error when images with lowest utility score estimated from gradient magnitudes are rejected. Furthermore, estimating FIQ by backpropagating  $\mathcal{L}_{\text{BNS}}$  yields significantly better results than using  $\text{MSE}_{\text{BNS}}$  directly.

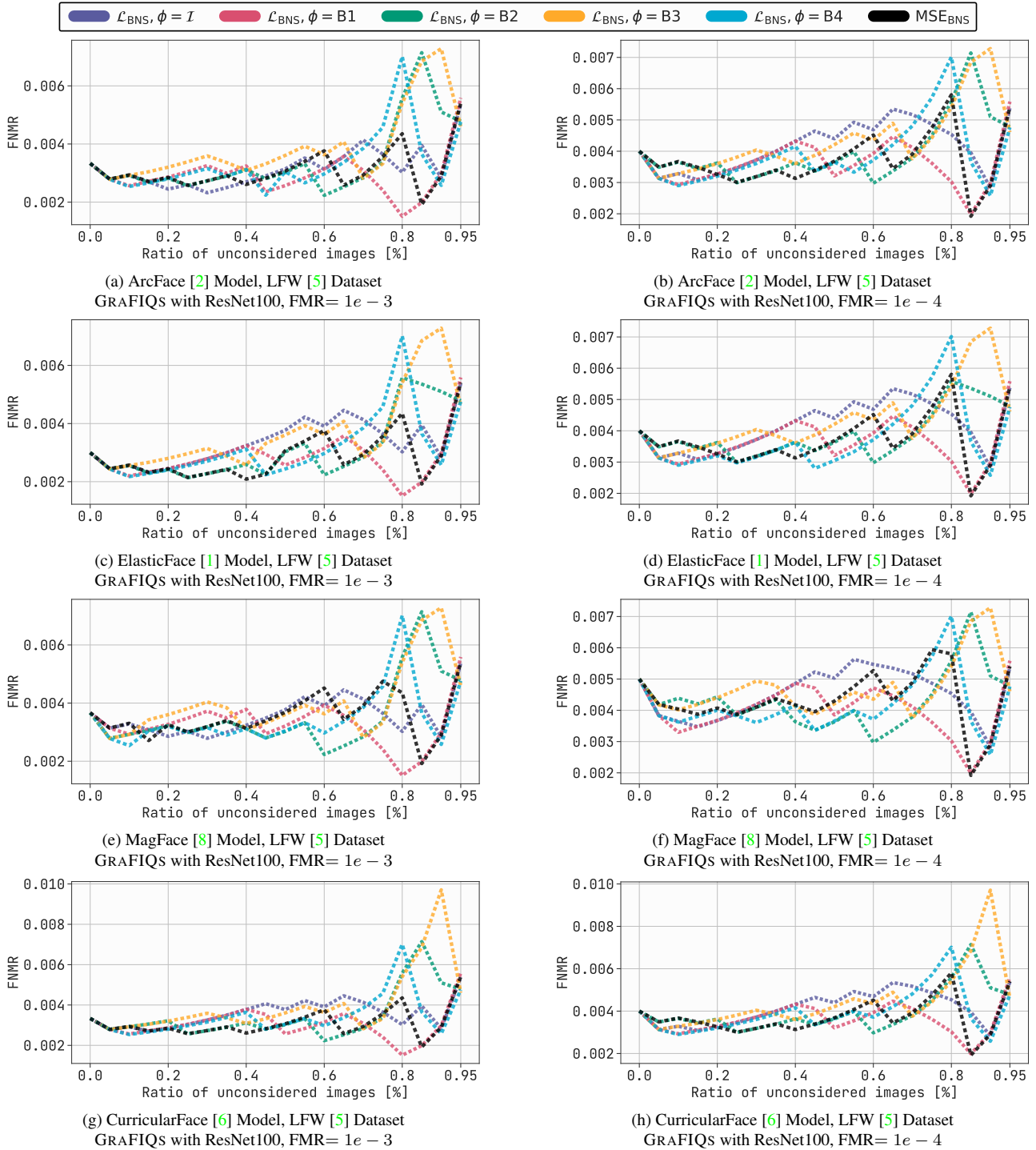


Figure 11. Error-versus-Discard Characteristic (EDC) curves for FNMR@FMR= $1e-3$  and FNMR@FMR= $1e-4$  of our proposed method using  $\mathcal{L}_{\text{BNS}}$  as backpropagation loss and absolute sum as FIQ. The gradients at image level ( $\phi = \mathcal{I}$ ), and block levels ( $\phi = \text{B1} - \phi = \text{B4}$ ) are used to calculate FIQ.  $\text{MSE}_{\text{BNS}}$  as FIQ is shown in black. Results shown on benchmark LFW [5] using ArcFace, ElasticFace, MagFace, and, CurricularFace FR models. It is evident that the proposed GRAFIQS method leads to lower verification error when images with lowest utility score estimated from gradient magnitudes are rejected. Furthermore, estimating FIQ by backpropagating  $\mathcal{L}_{\text{BNS}}$  yields significantly better results than using  $\text{MSE}_{\text{BNS}}$  directly.

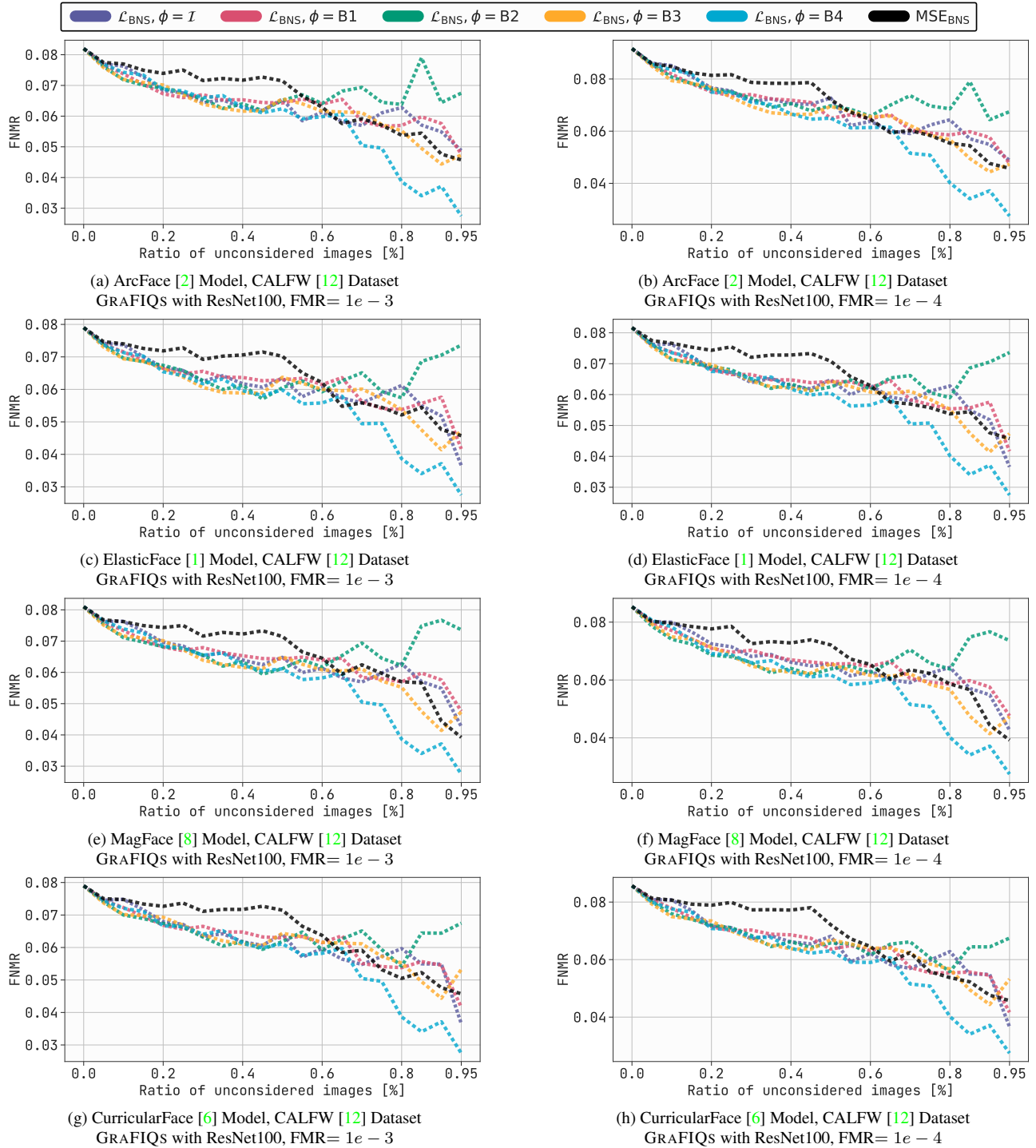


Figure 12. Error-versus-Discard Characteristic (EDC) curves for  $\text{FNMR}@FMR=1e-3$  and  $\text{FNMR}@FMR=1e-4$  of our proposed method using  $\mathcal{L}_{\text{BNS}}$  as backpropagation loss and absolute sum as FIQ. The gradients at image level ( $\phi = \mathcal{I}$ ), and block levels ( $\phi = \text{B1} - \phi = \text{B4}$ ) are used to calculate FIQ.  $\text{MSE}_{\text{BNS}}$  as FIQ is shown in black. Results shown on benchmark CALFW [12] using ArcFace, ElasticFace, MagFace, and, CurricularFace FR models. It is evident that the proposed GRAFIQS method leads to lower verification error when images with lowest utility score estimated from gradient magnitudes are rejected. Furthermore, estimating FIQ by backpropagating  $\mathcal{L}_{\text{BNS}}$  yields significantly better results than using  $\text{MSE}_{\text{BNS}}$  directly.

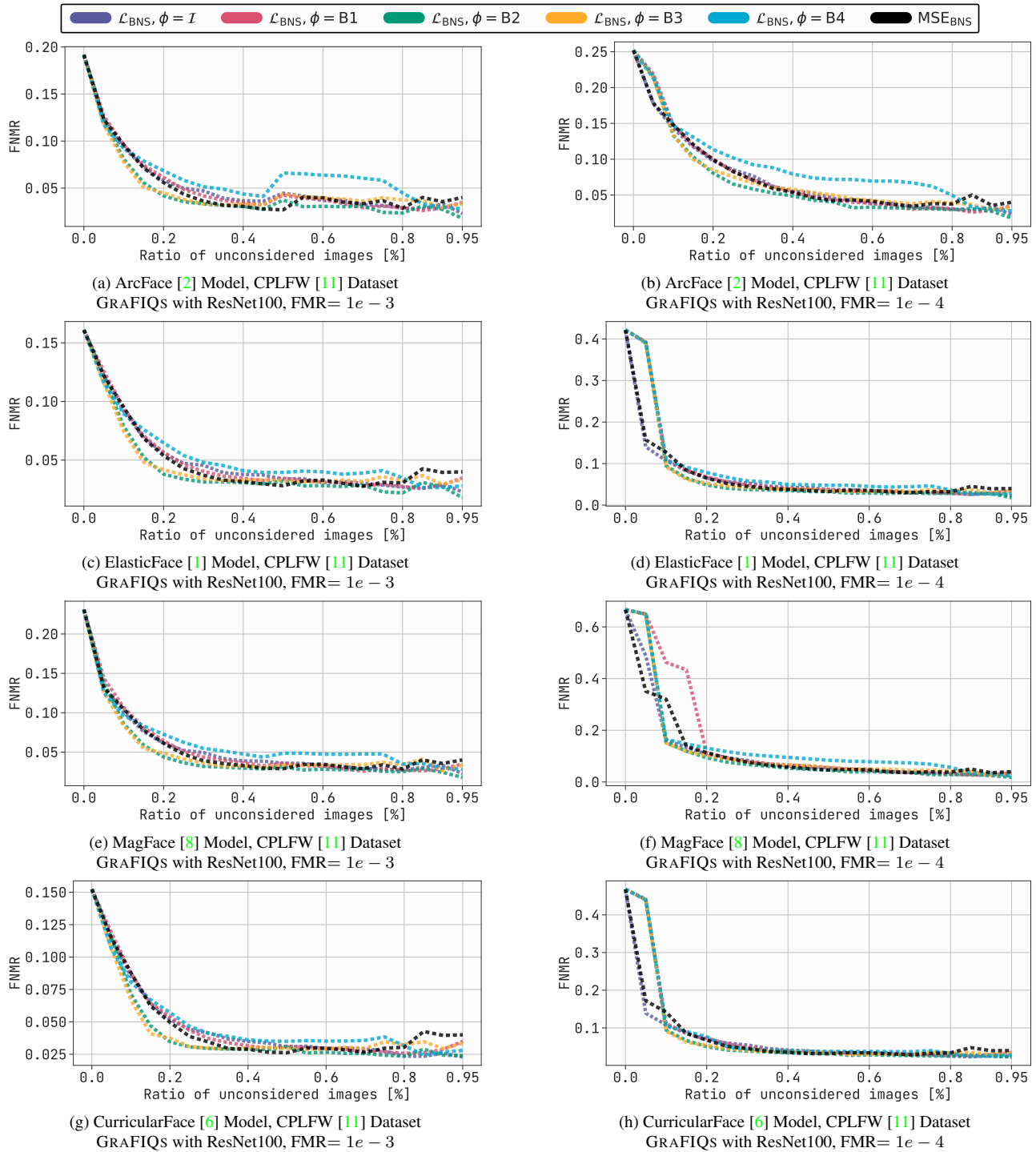


Figure 13. Error-versus-Discard Characteristic (EDC) curves for FNMR@FMR= $1e-3$  and FNMR@FMR= $1e-4$  of our proposed method using  $\mathcal{L}_{\text{BNS}}$  as backpropagation loss and absolute sum as FIQ. The gradients at image level ( $\phi = \mathcal{I}$ ), and block levels ( $\phi = \text{B1} - \phi = \text{B4}$ ) are used to calculate FIQ. MSE<sub>BNS</sub> as FIQ is shown in black. Results shown on benchmark CPLFW [11] using ArcFace, ElasticFace, MagFace, and, CurricularFace FR models. It is evident that the proposed GRAFIQS method leads to lower verification error when images with lowest utility score estimated from gradient magnitudes are rejected. Furthermore, estimating FIQ by backpropagating  $\mathcal{L}_{\text{BNS}}$  yields significantly better results than using MSE<sub>BNS</sub> directly.

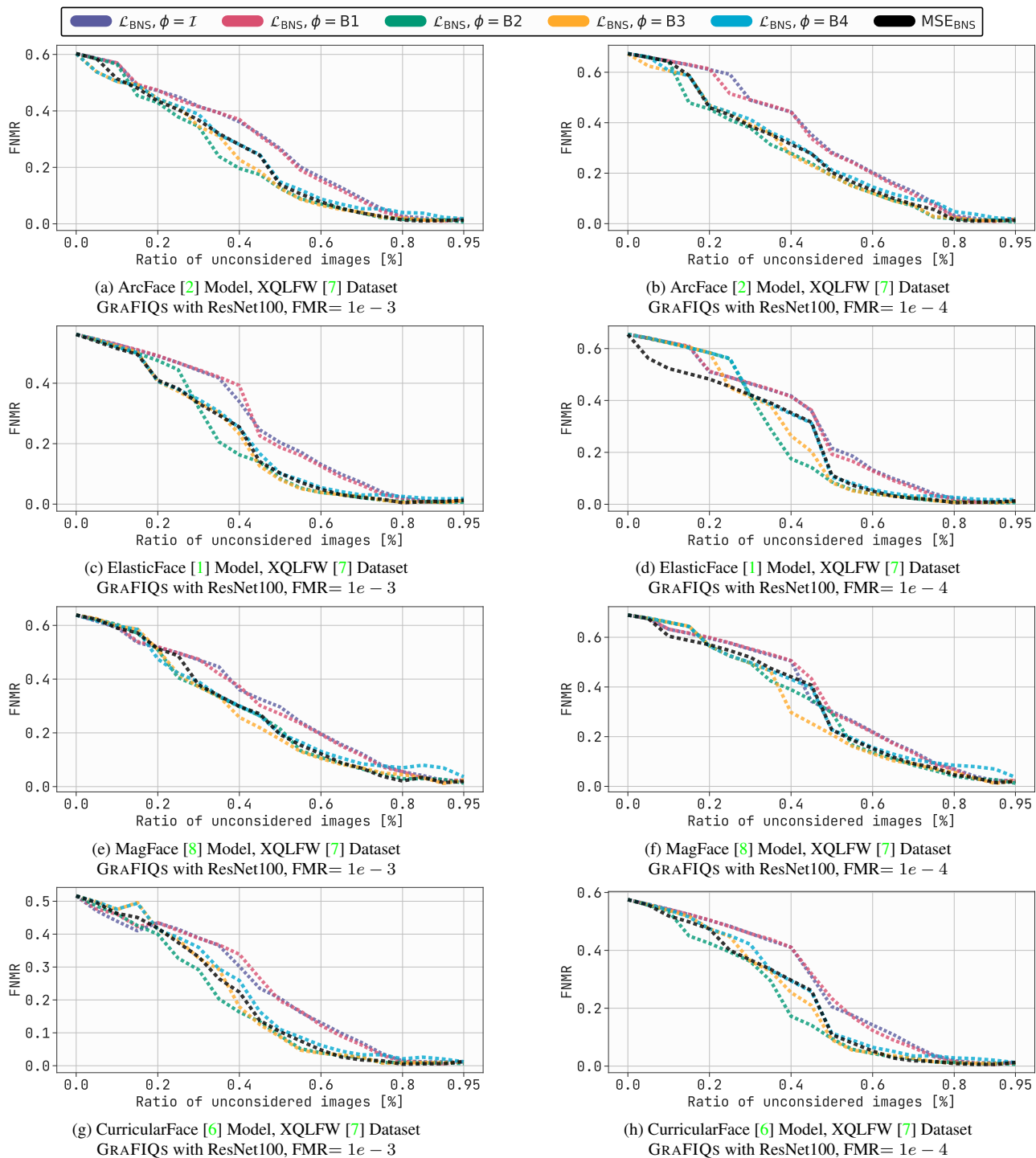


Figure 14. Error-versus-Discard Characteristic (EDC) curves for  $\text{FNMR}@FMR=1e-3$  and  $\text{FNMR}@FMR=1e-4$  of our proposed method using  $\mathcal{L}_{\text{BNS}}$  as backpropagation loss and absolute sum as FIQ. The gradients at image level ( $\phi = \mathcal{I}$ ), and block levels ( $\phi = \text{B1} - \phi = \text{B4}$ ) are used to calculate FIQ.  $\text{MSE}_{\text{BNS}}$  as FIQ is shown in black. Results shown on benchmark XQLFW [7] using ArcFace, ElasticFace, MagFace, and, CurricularFace FR models. It is evident that the proposed GRAFIQS method leads to lower verification error when images with lowest utility score estimated from gradient magnitudes are rejected. Furthermore, estimating FIQ by backpropagating  $\mathcal{L}_{\text{BNS}}$  yields significantly better results than using  $\text{MSE}_{\text{BNS}}$  directly.



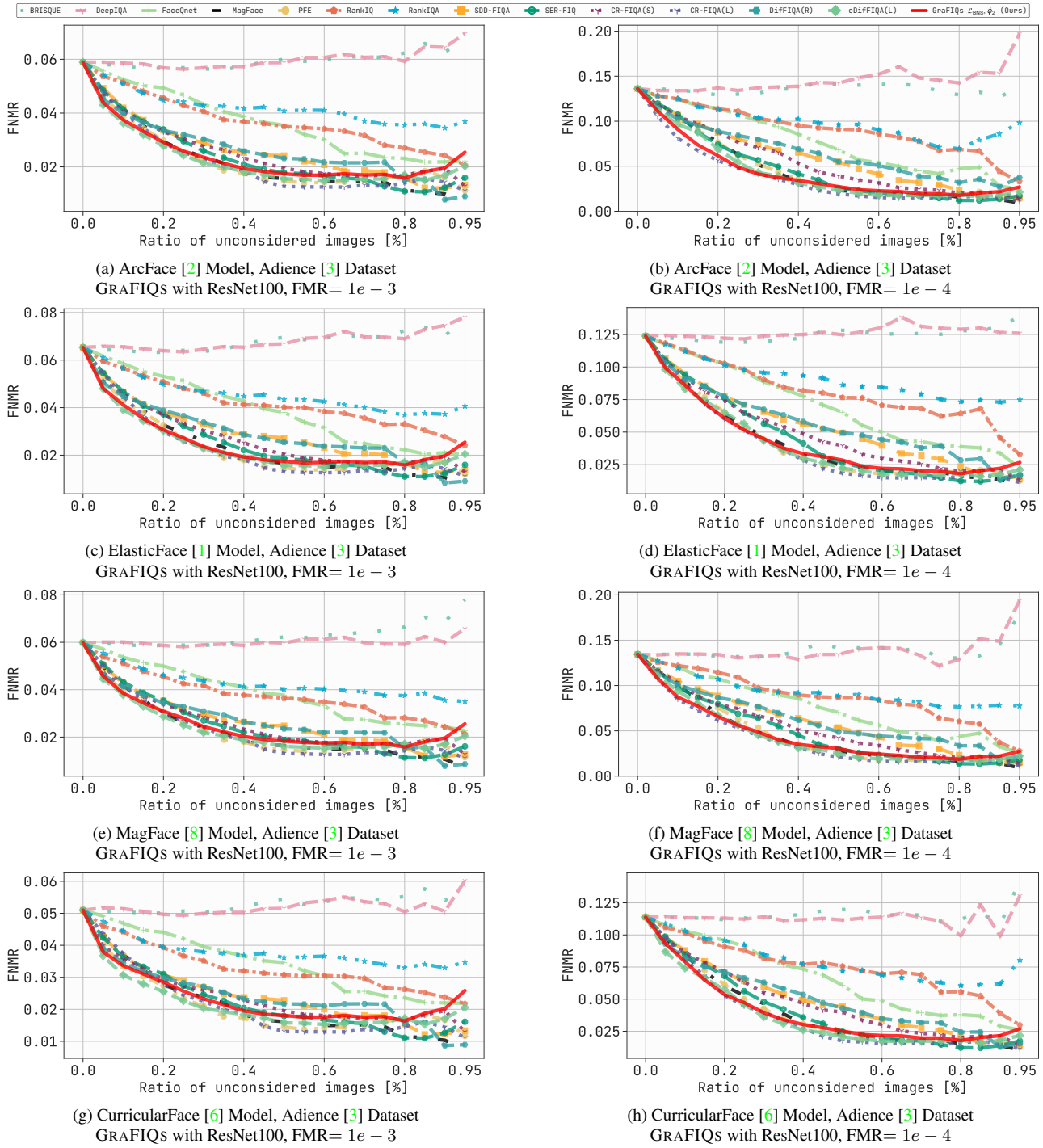


Figure 15. EDC curves for  $FNMR@FMR=1e-3$  and  $FNMR@FMR=1e-4$  on dataset Adience [3] using ArcFace, ElasticFace, MagFace, and CurricularFace FR models. The proposed GRAFIQs method, shown in solid red, utilizes gradient magnitudes and it is reported using the best setting from Table 2 in the main paper.

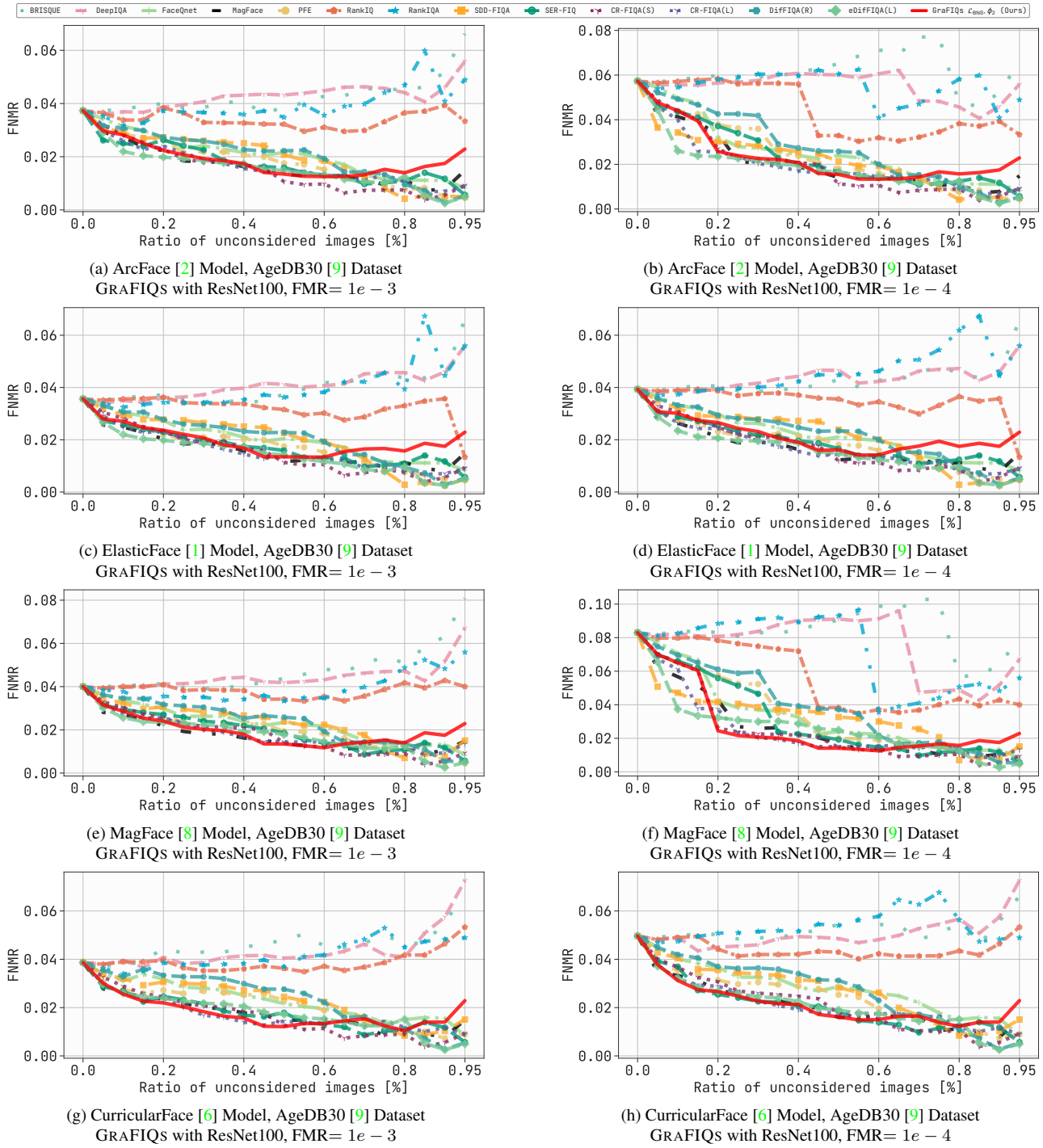


Figure 16. EDC curves for FNMR@FMR= $1e-3$  and FNMR@FMR= $1e-4$  on dataset AgeDB30 [9] using ArcFace, ElasticFace, MagFace, and CurricularFace FR models. The proposed GRAFIQs method, shown in solid red, utilizes gradient magnitudes and it is reported using the best setting from Table 2 in the main paper.

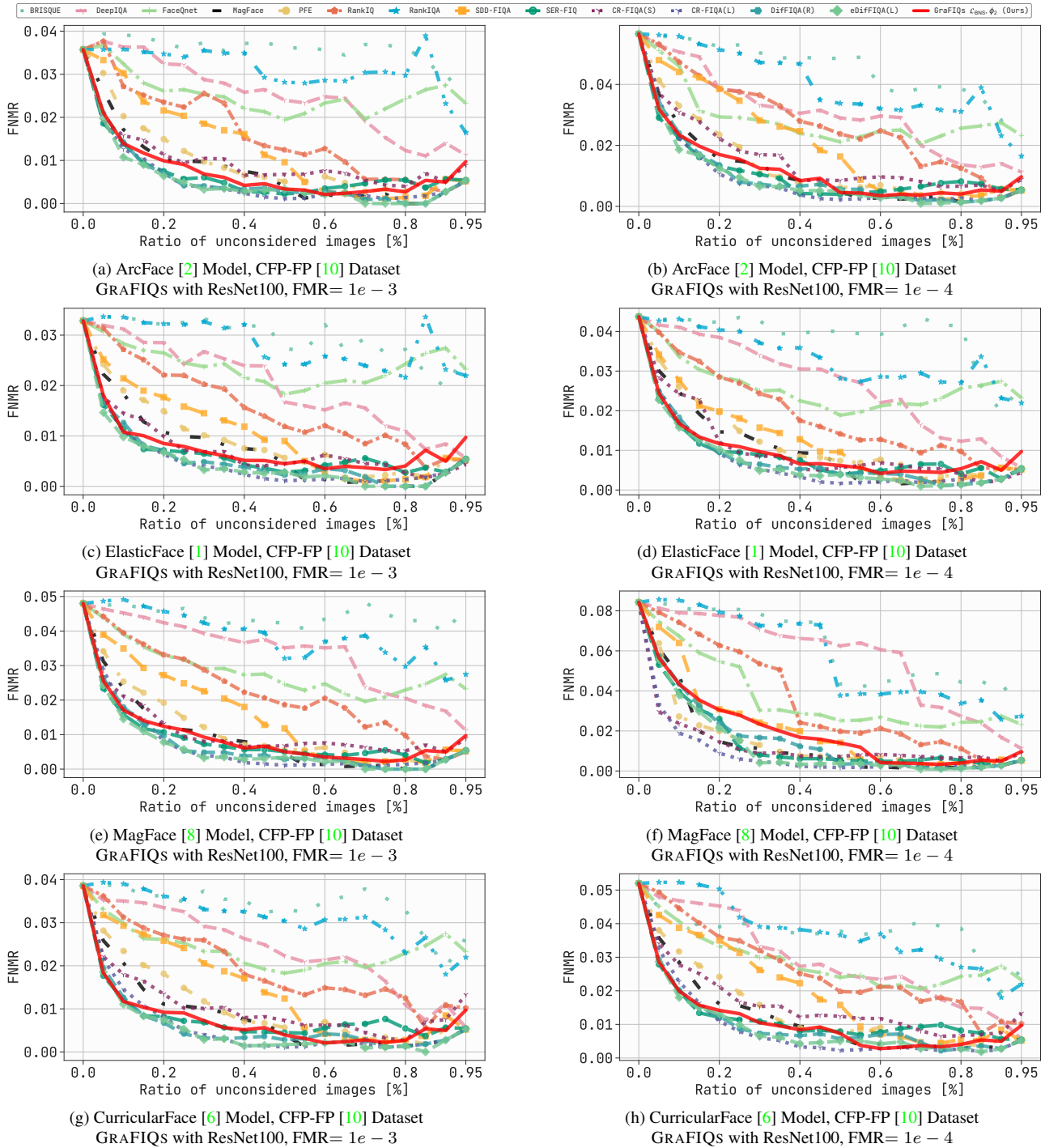


Figure 17. EDC curves for FNMR@FMR= $1e-3$  and FNMR@FMR= $1e-4$  on dataset CFP-FP [10] using ArcFace, ElasticFace, MagFace, and CurricularFace FR models. The proposed GRAFIQs method, shown in solid red, utilizes gradient magnitudes and it is reported using the best setting from Table 2 in the main paper.

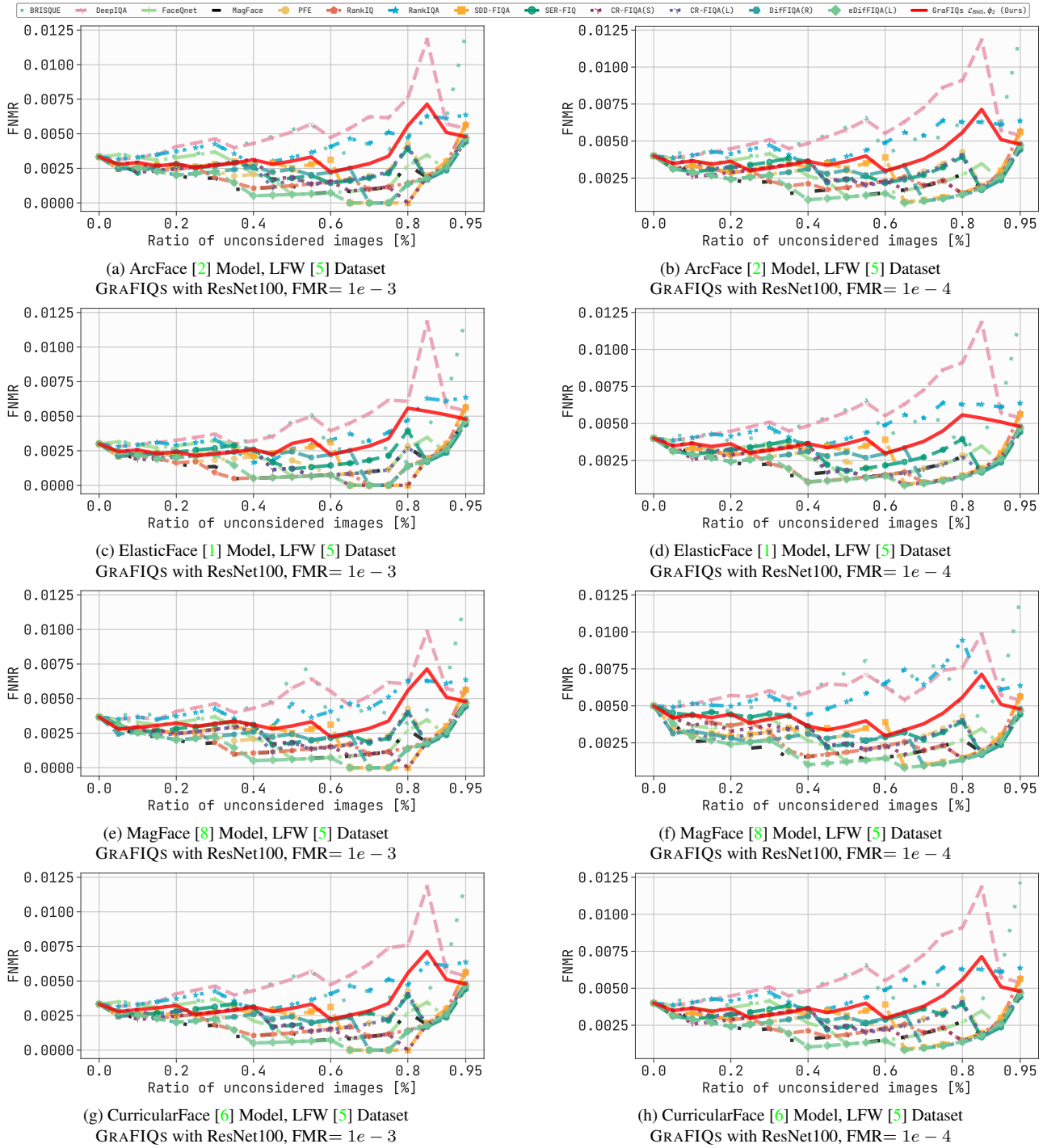


Figure 18. EDC curves for FNMR@FMR= $1e-3$  and FNMR@FMR= $1e-4$  on dataset LFW [5] using ArcFace, ElasticFace, MagFace, and CurricularFace FR models. The proposed GRAFIQs method, shown in solid red, utilizes gradient magnitudes and it is reported using the best setting from Table 2 in the main paper.

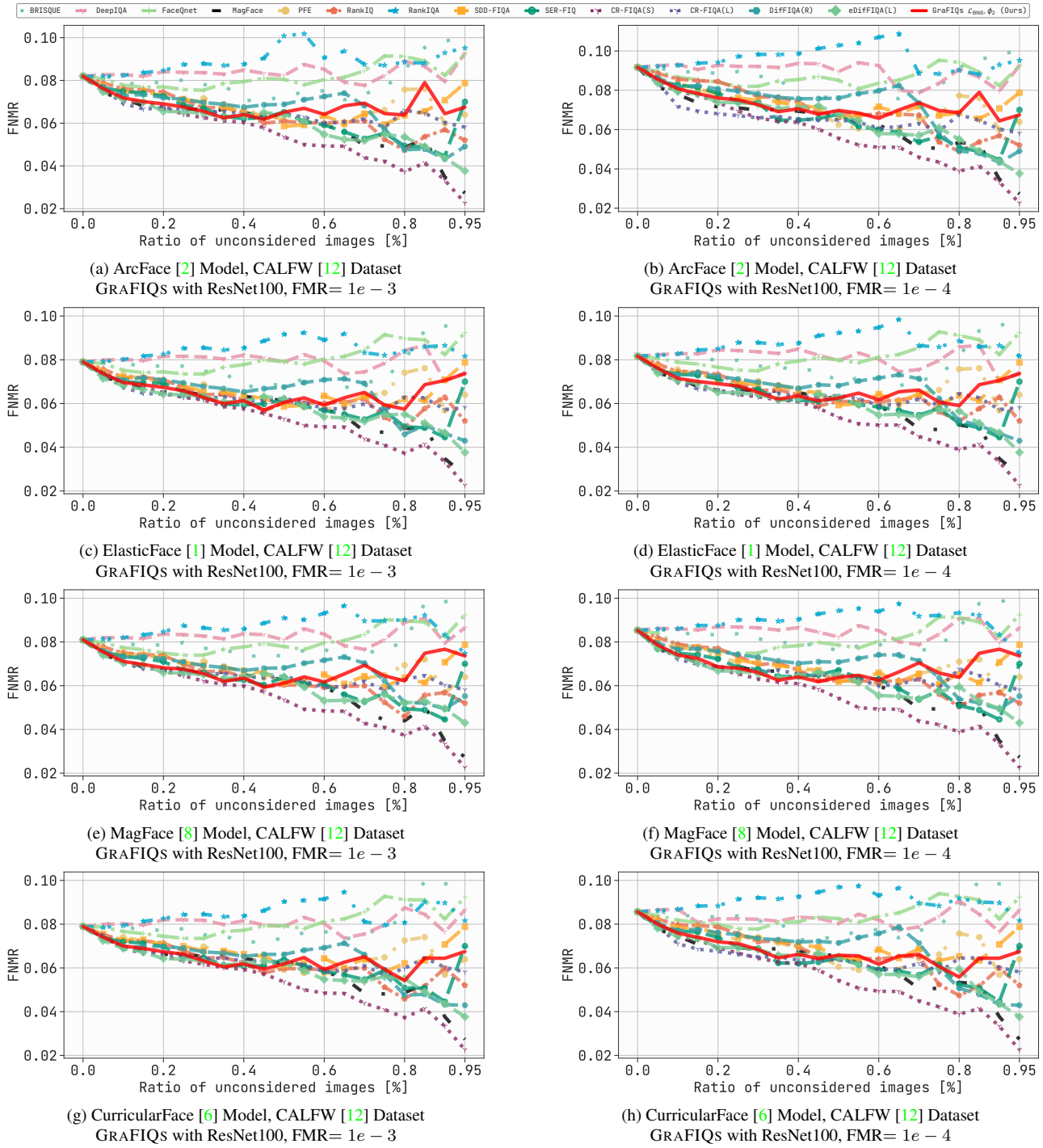


Figure 19. EDC curves for FNMR@FMR= $1e-3$  and FNMR@FMR= $1e-4$  on dataset CALFW [12] using ArcFace, ElasticFace, MagFace, and CurricularFace FR models. The proposed GRAFIQs method, shown in solid red, utilizes gradient magnitudes and it is reported using the best setting from Table 2 in the main paper.

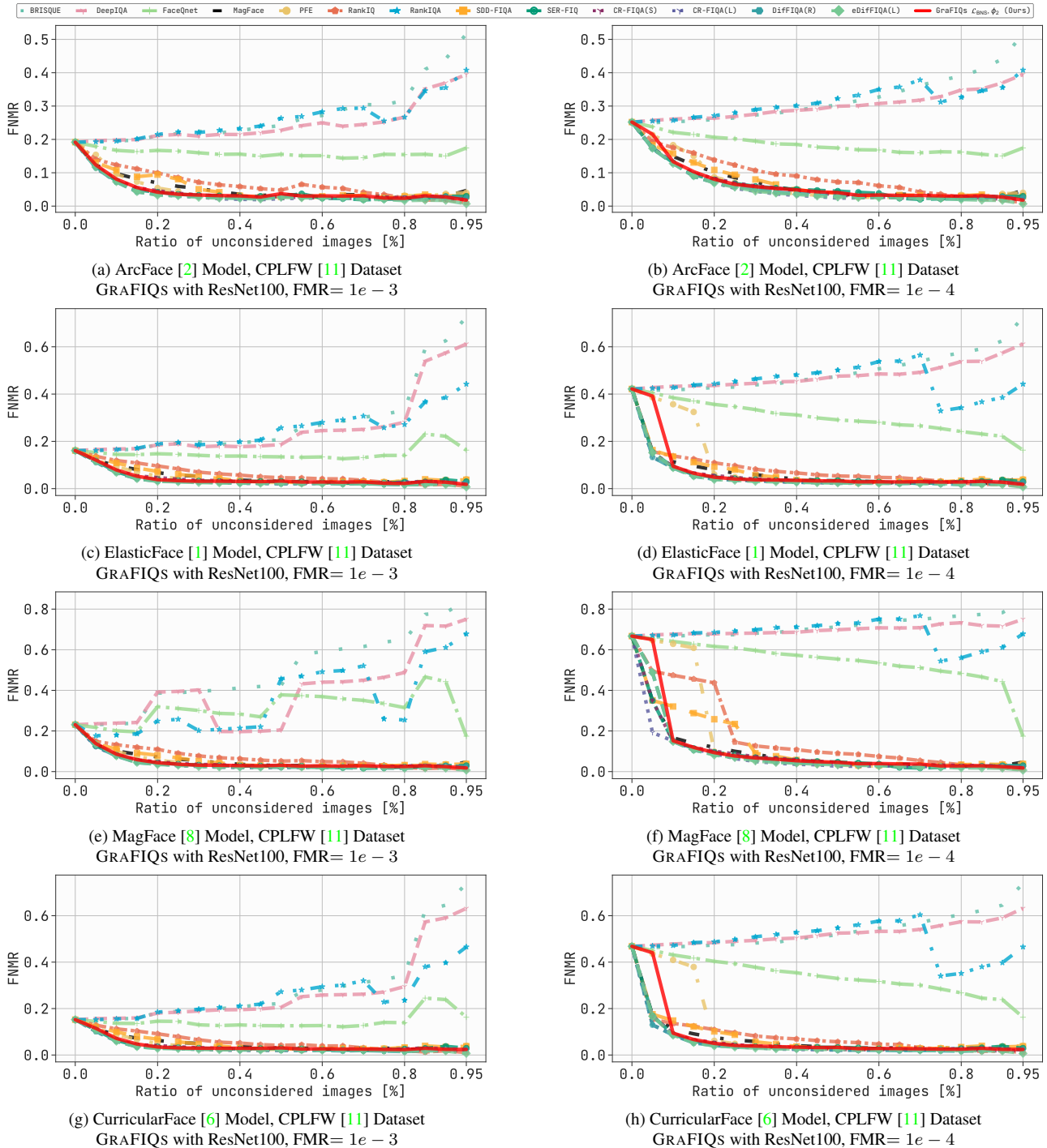


Figure 20. EDC curves for FNMR@FMR= $1e-3$  and FNMR@FMR= $1e-4$  on dataset CPLFW [11] using ArcFace, ElasticFace, MagFace, and CurricularFace FR models. The proposed GRAFIQs method, shown in solid red, utilizes gradient magnitudes and it is reported using the best setting from Table 2 in the main paper.

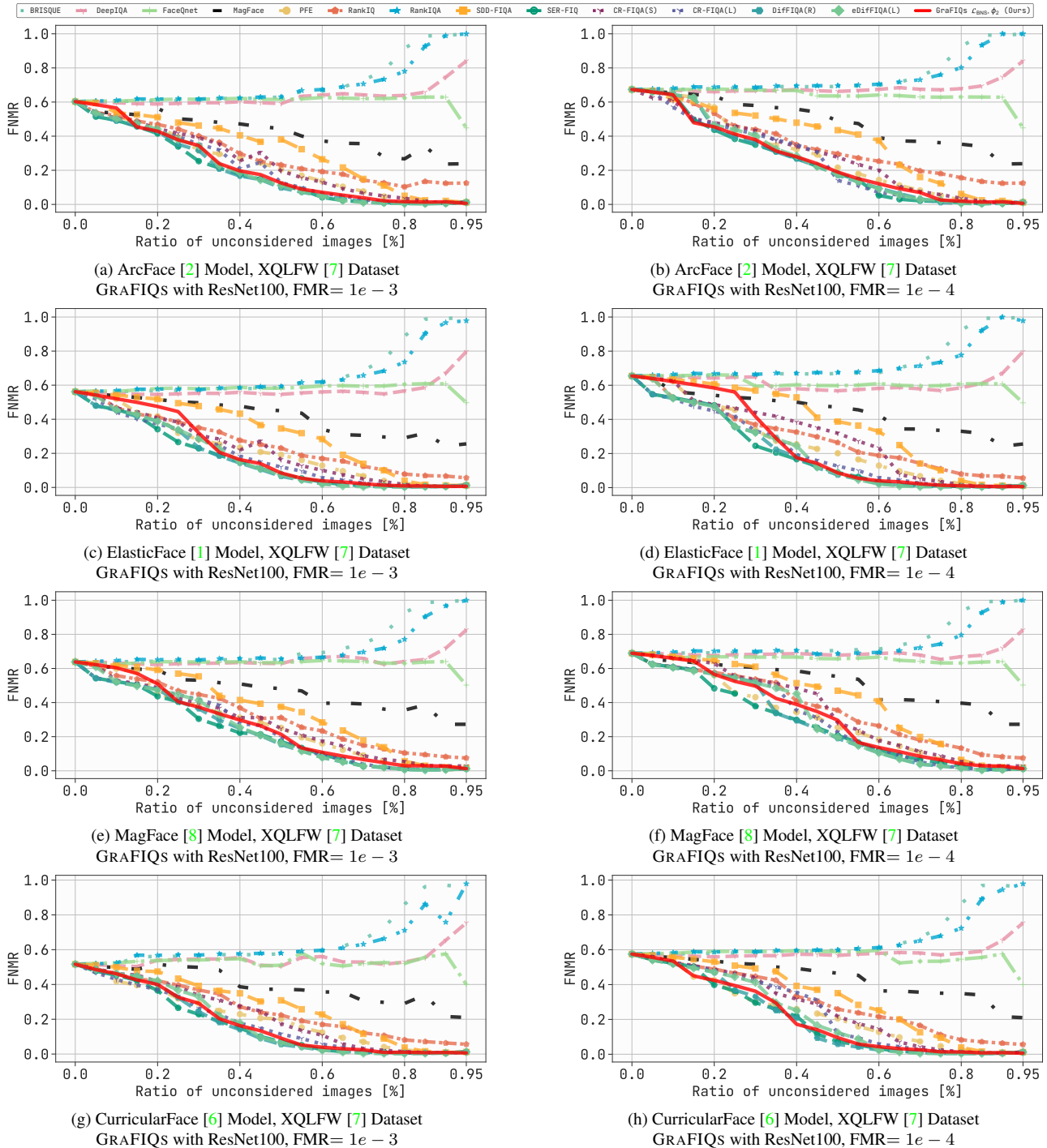


Figure 21. EDC curves for FNMR@FMR= $1e-3$  and FNMR@FMR= $1e-4$  on dataset XQLFW [7] using ArcFace, ElasticFace, MagFace, and CurricularFace FR models. The proposed GRAFIQS method, shown in solid red, utilizes gradient magnitudes and it is reported using the best setting from Table 2 in the main paper.

## References

- [1] Fadi Boutros, Naser Damer, Florian Kirchbuchner, and Arjan Kuijper. Elasticface: Elastic margin loss for deep face recognition. In *IEEE/CVF Conference on Computer Vision and Pattern Recognition Workshops, CVPR Workshops 2022, New Orleans, LA, USA, June 19-20, 2022*, pages 1577–1586. IEEE, 2022. [2](#), [3](#), [4](#), [5](#), [6](#), [7](#), [8](#), [9](#), [10](#), [11](#), [12](#), [13](#), [14](#), [15](#), [16](#), [17](#), [18](#), [19](#), [20](#), [21](#), [22](#), [23](#)
- [2] Jiankang Deng, Jia Guo, Niannan Xue, and Stefanos Zafeiriou. Arcface: Additive angular margin loss for deep face recognition. In *IEEE Conference on Computer Vision and Pattern Recognition, CVPR 2019, Long Beach, CA, USA, June 16-20, 2019*, pages 4690–4699. Computer Vision Foundation / IEEE, 2019. [2](#), [3](#), [4](#), [5](#), [6](#), [7](#), [8](#), [9](#), [10](#), [11](#), [12](#), [13](#), [14](#), [15](#), [16](#), [17](#), [18](#), [19](#), [20](#), [21](#), [22](#), [23](#)
- [3] Eran Eidinger, Roeen Enbar, and Tal Hassner. Age and gender estimation of unfiltered faces. *IEEE Trans. Inf. Forensics Secur.*, 9(12):2170–2179, 2014. [2](#), [3](#), [10](#), [17](#)
- [4] Kaiming He, Xiangyu Zhang, Shaoqing Ren, and Jian Sun. Deep residual learning for image recognition. In *2016 IEEE Conference on Computer Vision and Pattern Recognition, CVPR 2016, Las Vegas, NV, USA, June 27-30, 2016*, pages 770–778. IEEE Computer Society, 2016. [1](#)
- [5] Gary B. Huang, Manu Ramesh, Tamara Berg, and Erik Learned-Miller. Labeled faces in the wild: A database for studying face recognition in unconstrained environments. Technical Report 07-49, University of Massachusetts, Amherst, October 2007. [2](#), [6](#), [13](#), [20](#)
- [6] Yuge Huang, Yuhan Wang, Ying Tai, Xiaoming Liu, Pengcheng Shen, Shaoxin Li, Jilin Li, and Feiyue Huang. Curricularface: Adaptive curriculum learning loss for deep face recognition. In *2020 IEEE/CVF Conference on Computer Vision and Pattern Recognition, CVPR 2020, Seattle, WA, USA, June 13-19, 2020*, pages 5900–5909. Computer Vision Foundation / IEEE, 2020. [2](#), [3](#), [4](#), [5](#), [6](#), [7](#), [8](#), [9](#), [10](#), [11](#), [12](#), [13](#), [14](#), [15](#), [16](#), [17](#), [18](#), [19](#), [20](#), [21](#), [22](#), [23](#)
- [7] Martin Knoche, Stefan Hörmann, and Gerhard Rigoll. Cross-quality LFW: A database for analyzing cross-resolution image face recognition in unconstrained environments. In *16th IEEE International Conference on Automatic Face and Gesture Recognition, FG 2021, Jodhpur, India, December 15-18, 2021*, pages 1–5. IEEE, 2021. [2](#), [9](#), [16](#), [23](#)
- [8] Qiang Meng, Shichao Zhao, Zhida Huang, and Feng Zhou. Magface: A universal representation for face recognition and quality assessment. In *IEEE Conference on Computer Vision and Pattern Recognition, CVPR 2021, virtual, June 19-25, 2021*, pages 14225–14234. Computer Vision Foundation / IEEE, 2021. [2](#), [3](#), [4](#), [5](#), [6](#), [7](#), [8](#), [9](#), [10](#), [11](#), [12](#), [13](#), [14](#), [15](#), [16](#), [17](#), [18](#), [19](#), [20](#), [21](#), [22](#), [23](#)
- [9] Stylianos Moschoglou, Athanasios Papaioannou, Christos Sagonas, Jiankang Deng, Irene Kotsia, and Stefanos Zafeiriou. Agedb: The first manually collected, in-the-wild age database. In *2017 IEEE CVPRW, CVPR Workshops 2017, Honolulu, HI, USA, July 21-26, 2017*, pages 1997–2005. IEEE Computer Society, 2017. [2](#), [4](#), [11](#), [18](#)
- [10] Soumyadip Sengupta, Jun-Cheng Chen, Carlos Domingo Castillo, Vishal M. Patel, Rama Chellappa, and David W. Jacobs. Frontal to profile face verification in the wild. In *2016 IEEE Winter Conference on Applications of Computer Vision, WACV 2016, Lake Placid, NY, USA, March 7-10, 2016*, pages 1–9. IEEE Computer Society, 2016. [2](#), [5](#), [12](#), [19](#)
- [11] T. Zheng and W. Deng. Cross-pose lfw: A database for studying cross-pose face recognition in unconstrained environments. Technical Report 18-01, Beijing University of Posts and Telecommunications, February 2018. [2](#), [8](#), [15](#), [22](#)
- [12] Tianyue Zheng, Weihong Deng, and Jiani Hu. Cross-age LFW: A database for studying cross-age face recognition in unconstrained environments. *CoRR*, abs/1708.08197, 2017. [2](#), [7](#), [14](#), [21](#)